Simulated Seizures and Spreading Depression in a Neuron Model Incorporating Interstitial Space and Ion Concentrations

H. KAGER,[1] W. J. WADMAN,[1] AND G. G. SOMJEN[2]
[1]*Institute of Neurobiology, University of Amsterdam, 1098 SM Amsterdam, The Netherlands; and* [2]*Department of Cell Biology, Duke University Medical Center, Durham, North Carolina 27710*

Received 1 November 1999; accepted in final form 20 March 2000

Kager, H., W. J. Wadman, and G. G. Somjen. Simulated seizures and spreading depression in a neuron model incorporating interstitial space and ion concentrations. *J Neurophysiol* 84: 495–512, 2000. Sustained inward currents in neuronal membranes underlie tonic-clonic seizure discharges and spreading depression (SD). It is not known whether these currents flow through abnormally operating physiological ion channels or through pathological pathways that are not normally present. We have now used the NEURON simulating environment of Hines, Moore, and Carnevale to model seizure discharges and SD. The geometry and electrotonic properties of the model neuron conformed to a hippocampal pyramidal cell. Voltage-controlled transient and persistent sodium currents ($I_{Na,T}$ and $I_{Na,P}$), potassium currents ($I_{K,DR}$ and $I_{K,A}$), and *N*-methyl-D-aspartate (NMDA) receptor-controlled currents (I_{NMDA}), were inserted in the appropriate regions of the model cell. The neuron was surrounded by an interstitial space where extracellular potassium and sodium concentration ($[K^+]_o$ and $[Na^+]_o$) could rise or fall. Changes in intra- and extracellular ion concentrations and the resulting shifts in the driving force for ionic currents were continuously computed based on the amount of current flowing through the membrane. A Na-K exchange pump operated to restore ion balances. In addition, extracellular potassium concentration, $[K^+]_o$, was also controlled by a "glial" uptake function. Parameters were chosen to resemble experimental data. As long as $[K^+]_o$ was kept within limits by the activity of the Na-K pump and the "glial" uptake, a depolarizing current pulse applied to the cell soma evoked repetitive firing that ceased when the stimulating current stopped. If, however, $[K^+]_o$ was allowed to rise, then a brief pulse provoked firing that outlasted the stimulus. At the termination of such a burst, the cell hyperpolarized and then slowly depolarized and another burst erupted without outside intervention. Such "clonic" bursting could continue indefinitely maintained by an interplay of the rise and fall of potassium and sodium concentrations with membrane currents and threshold levels. SD-like depolarization could be produced in two ways, *1*) by a dendritic NMDA-controlled current. Glutamate was assumed to be released in response to rising $[K^+]_o$. And *2*) by the persistent (i.e., slowly inactivating) Na-current, $I_{Na,P}$. When both I_{NMDA} and $I_{Na,P}$ were present, the two acted synergistically. We conclude that epileptiform neuronal behavior and SD-like depolarization can be generated by the feedback of ion currents that change ion concentrations, which, in turn, influence ion currents and membrane potentials. The normal stability of brain function must depend on the efficient control of ion activities, especially that of $[K^+]_o$.

INTRODUCTION

The electrophysiology of epileptiform seizures has been studied since the early 1930s and the phenomenon of spreading depression (SD) was discovered by Leão in the 1940s (Leão 1944). The extra- and intracellular electrical signs and the ion concentration changes accompanying these processes have been described in some detail (Bureš et al. 1974; Heinemann et al. 1978; Marshall 1959; Nicholson 1984; Somjen et al. 1986), yet the biophysical mechanisms underlying these phenomena are not completely understood. During the tonic phase of an epileptic seizure, large numbers of neurons are firing, the discharge being driven by steady depolarization. Gloor et al. (1961, 1964) have shown that in the hippocampal formation, tonic discharge is accompanied by a negative shift of the extracellular potential, V_o, that is limited to the cell body layers and is usually accompanied by a positive shift of potential in layers containing mostly neuron dendrites and neuroglia. Unlike in neocortex and spinal cord, in the hippocampal formation, the contribution of glia to extracellular potential shifts is negligible (reviewed by Somjen 1995). We have confirmed the distribution of V_o shifts during seizures, and we have also shown that the seizure-related rise in extracellular potassium concentration, $[K^+]_o$, is maximal in cell body layers (Somjen and Giacchino 1985; Somjen et al. 1985). Current source density analysis then revealed a current sink limited to cell soma layers that persisted as long as the seizure continued. By contrast, during SD, current source density maps show very large inward currents in the zones of dendritic trees (Wadman et al. 1992). Unlike during seizures, during SD, the membrane potential measured in neuron somata is reduced to between 0 and −20 mV and firing ceases. The cell input resistance measured with sharp electrodes in current clamp drops to less than 12% of its normal value (Czéh et al. 1993; Müller and Somjen 1998, 2000; Schwartzkroin 1984; Snow et al. 1983).

In spite of the obvious differences between seizures and SD, there are also important similarities. Both seizures and SD can be triggered by similar insults, and both are inhibited by similar physical or pharmacological interventions, such as cooling, hypertonicity, acidosis, and certain depressant drugs (Bureš et al. 1974; Marshall 1959). An event that begins with an epileptiform discharge can sometimes terminate in SD (Somjen and Aitken 1984), and a seizure that starts in a focus can then

Address for reprint requests: G. Somjen, Dept. of Cell Biology, Duke University Medical Center, Box 3709, Durham, NC 27710 (E-mail: g.somjen@cellbio.duke.edu).

The costs of publication of this article were defrayed in part by the payment of page charges. The article must therefore be hereby marked "*advertisement*" in accordance with 18 U.S.C. Section 1734 solely to indicate this fact.

 0022-3077/00 $5.00 Copyright © 2000 The American Physiological Society

Downloaded from www.physiology.org/journal/jn by ${individualUser.givenNames} ${individualUser.surname} (129.034.020.019) on December 28, 2017.
Copyright © 2000 American Physiological Society. All rights reserved.

spread over a large area with a velocity resembling that of SD (Bureš et al. 1974; Van Harreveld and Stamm 1953). Finally, intense, persistent inward currents characterize both processes, albeit differently distributed over the neuron surface (Wadman et al. 1992).

Neither for tonic-clonic seizures nor for SD have the channels been identified that drive the persistent depolarization. Hypothetically the depolarizing current could be generated by the abnormal operation of one or more of the known physiological membrane channels or it could involve ion flow through pathways that are not normally present. Pharmacological blockade of some of the known ion channels delays SD, shortens its duration, and reduces the amplitude of the associated depolarization, but none could completely prevent it (Bureš et al. 1984; Hernández-Cáceres et al. 1987; Herreras and Somjen 1993a; Marrannes et al. 1993). This failure seemed to favor the idea that SD is caused by the opening of a pathological pathway for ion flow that is not normally present in the membrane. Recently, however, Müller and Somjen (1998) found that simultaneous blockade of all known major inward currents did prevent hypoxia-induced SD-like depolarization. This observation could mean that the depolarization is generated by the cooperative action of several channels, and this could explain why blocking any one of the channels can slow down the process or curtail its intensity but not stop it.

To test this hypothesis, we now used computer simulation to examine whether, under the appropriate conditions, the activation of physiological channels could produce SD-like depolarization. The results of the computations suggest that this is indeed possible. In the course of the trials, we discovered that the model could also behave in ways resembling discharges that are recorded from neurons during some forms of epileptic seizures. The key to both classes of pathological behavior appears to be positive feedback loops in which ion currents produce ion concentration changes, which, in turn, profoundly alter ion currents.

An abstract of some of these results is in Somjen et al. (2000).

METHODS

All simulations were run in the NEURON modeling environment designed by Hines, Moore, and Carnevale for simulating electrical behavior of branched neuronal structures (Hines and Carnevale 1997).

Morphology

Several series of experiments were run on reduced neurons, which consisted either of a single somatic compartment or a soma with sparsely branched dendritic loads attached. However, we illustrate in this report our findings using a model cell with morphology based on reconstruction of a hippocampal CA1 neuron of a young adult rat. This is *cell n408* from the Duke-Southampton Archive of Neuronal Morphology (Cannon et al. 1998; Pyapali et al. 1998) (Fig. 1*A* and Table 1). This neuron was represented in 201 electrically coupled compartments. For simplification we have assumed membrane parameters that were identical in all dendritic compartments but distinct from those of the somatic compartment. In text Figs. 3–10, we illustrate the variables that were recorded from the somatic compartment, a proximal dendritic compartment and a distal dendritic compartment (see Fig. 1, d2 and d14). The electrical parameters were in part similar to those of the hippocampal neuron model of Traub et al. (1994), and in part they were based on data obtained from hippocampal preparations in our laboratories.

Passive electrical properties

The model did not incorporate the axon nor dendritic spines. Spatial discretization of the numerical compartments was chosen so that no compartment was longer than 0.2 electrotonic lengths (Rall et al. 1992). With a specific membrane capacitance C_m of 0.75 μF/cm^2, the total membrane capacity of the cell became 212 pF. The axial resistivity was set to 100 Ω*cm. Resting sodium and potassium permeabilities were then used to define the input resistance and resting membrane potential. With a sodium leak conductance of $2 * 10^{-5}$ S/cm^2 and a potassium leak conductance of $7 * 10^{-5}$ S/cm^2, we obtained an input resistance of 100 MΩ and a membrane resting potential near to -70 mV. In the following simulations we added a fixed leak of $20 * 10^{-5}$ S/cm^2 with a reversal potential set to -70 mV to stabilize the membrane potential and reduce the input resistance to between 50 and 100 MΩ

$$I_{\text{leak,Na}} = g_{\text{leak,Na}} * (V - E_{\text{Na}})$$

$$I_{\text{leak,K}} = g_{\text{leak,K}} * (V - E_{\text{K}})$$

$$I_{\text{leak,f}} = g_{\text{leak,f}} * (V + 70)$$

Active membrane conductances

The voltage-dependent sodium and potassium conductances were simulated using the classical Hodgkin and Huxley kinetic description (Hille 1992; Hodgkin and Huxley 1952). The expressions used for the rate constants that describe the voltage-dependent transition of the first order m and h gate are based on a model of hippocampal pyramidal cells described by Traub et al. (1994). The Goldman-Hodgkin-Katz equation (GHK) was used to describe the current-voltage relation for each ionic current as a function of absolute membrane potential V

$$I_{\text{GHK}}([\text{Ion}]_i, [\text{Ion}]_o, V) = V * z\alpha F * P_0 * \frac{[\text{Ion}]_i - [\text{Ion}]_o \exp(-\alpha V)}{1 - \exp(-\alpha V)}$$

with

$$\alpha = \frac{zF}{RT}$$

where P_0 is the membrane permeability, F is Faraday's constant, R is the gas constant, T is the absolute temperature, and z is the valence of the current carrying ion. The temperature was set to 37°C. The generalized formula for each active current can now be written as

$$I_{\text{Ion}}(V, t) = g_{\text{max}} * \text{Gates}\{m(V, t), h(V, t)\} * \text{GHK}\{[\text{Ion}]_i, [\text{Ion}]_o, V\}$$

where "gates" (m, h) describe the dependence of the current on the activation and/or inactivation gates. Five active membrane currents were incorporated.

Transient Na current, $I_{Na,T}$

The fast transient sodium current, $I_{\text{Na,T}}$ was inserted only in the somatic compartment. We used the description given by Traub et al. (1994), but based on our own observations (Vreugdenhil et al. 1998), we shifted the activation function 5 mV in depolarizing direction. This slightly increased the threshold for action potentials and reduced the "window" current (Fig. 2, *A* and *B*). The following equation relates the membrane current to the gating

$$I_{\text{Na,T}} = g_{\text{Na,T}} * m^3 * h * \text{GHK}(\text{Na}_i, \text{Na}_o, V)$$

Downloaded from www.physiology.org/journal/jn by ${individualUser.givenNames} ${individualUser.surname} (129.034.020.019) on December 28, 2017.
Copyright © 2000 American Physiological Society. All rights reserved.

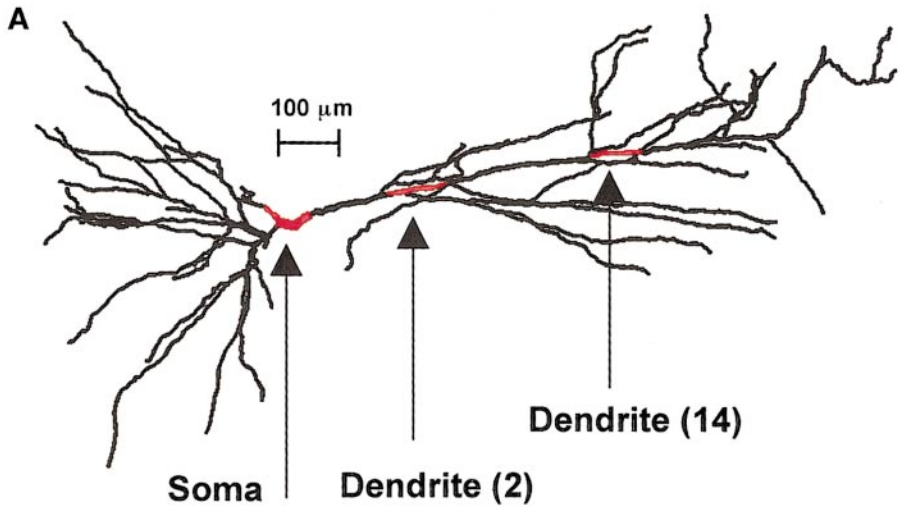

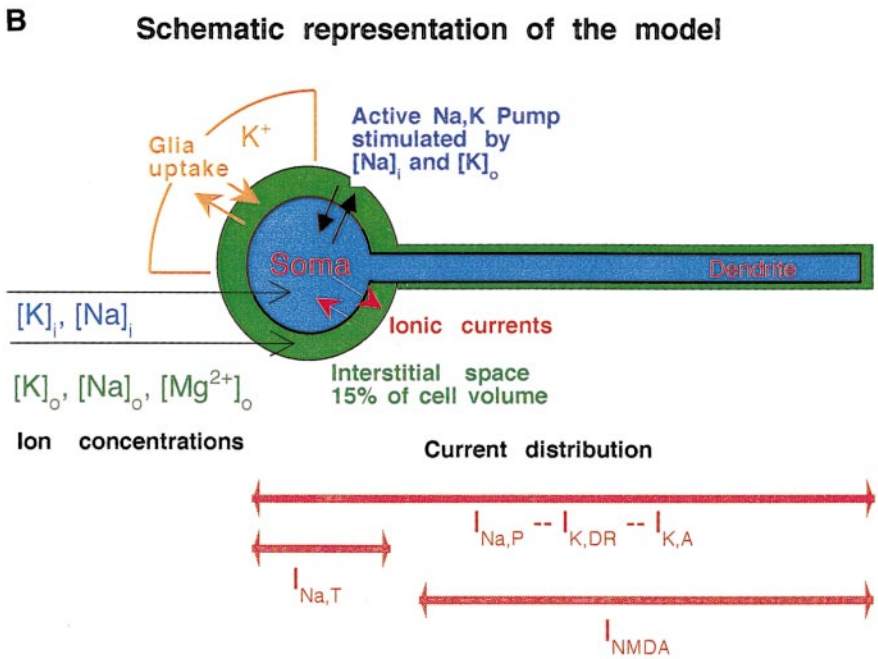

FIG. 1. *A*: the geometry of the model neuron. ↑, the regions from which recordings are illustrated in Figs. 3–10: dendrite (2) is the second, dendrite (14) is the 14th dendritic segment. The computations were based on the responses of the entire neuron. The model is based on a CA1 pyramidal cell, published in the Duke-Southampton Archive of Neuronal Morphology (Cannon et al. 1998). *B*: schema of the main constituents of the model: currents, fluxes and concentrations. The drawing in *B* is not to scale.

where $g_{Na,T}$ was the conductance at maximal activation, and it was usually set to about 100 * 10^{-5} S/cm^2. The forward (α) and the backward (β) rate constants describe the transition between the closed and open state of the first-order activation gate, *m*

TABLE 1. *Morphological parameters of the model cell*

	Soma	Apical	Basal
Cell geometry			
Total surface, μm^2	1,586	16,408	10,324
Total volume, μm^3	2,160	3,852	1,762
For the compartments illustrated			
	Soma	Proximal (d2)	Distal (d14)
Surface/volume	0.73	1.89	2.26

$$\alpha_m = 0.32 * \frac{-V - 51.9}{\exp - (0.25 * V + 12.975) - 1}$$

and

$$\beta_m = 0.28 * \frac{V + 24.89}{\exp(0.2 * V + 4.978) - 1}$$

as well as for the inactivation gate *h*

$$\alpha_h = 0.128 * \exp - (0.056 * V + 2.94)$$

and

$$\beta_h = \frac{4}{1 + \exp - (0.2 * V + 6)}$$

To illustrate the properties of some of the simulated currents, Fig. 2, *A* and *B*, shows sodium currents computed in voltage-clamp mode

Downloaded from www.physiology.org/journal/jn by ${individualUser.givenNames} ${individualUser.surname} (129.034.020.019) on December 28, 2017.
Copyright © 2000 American Physiological Society. All rights reserved.

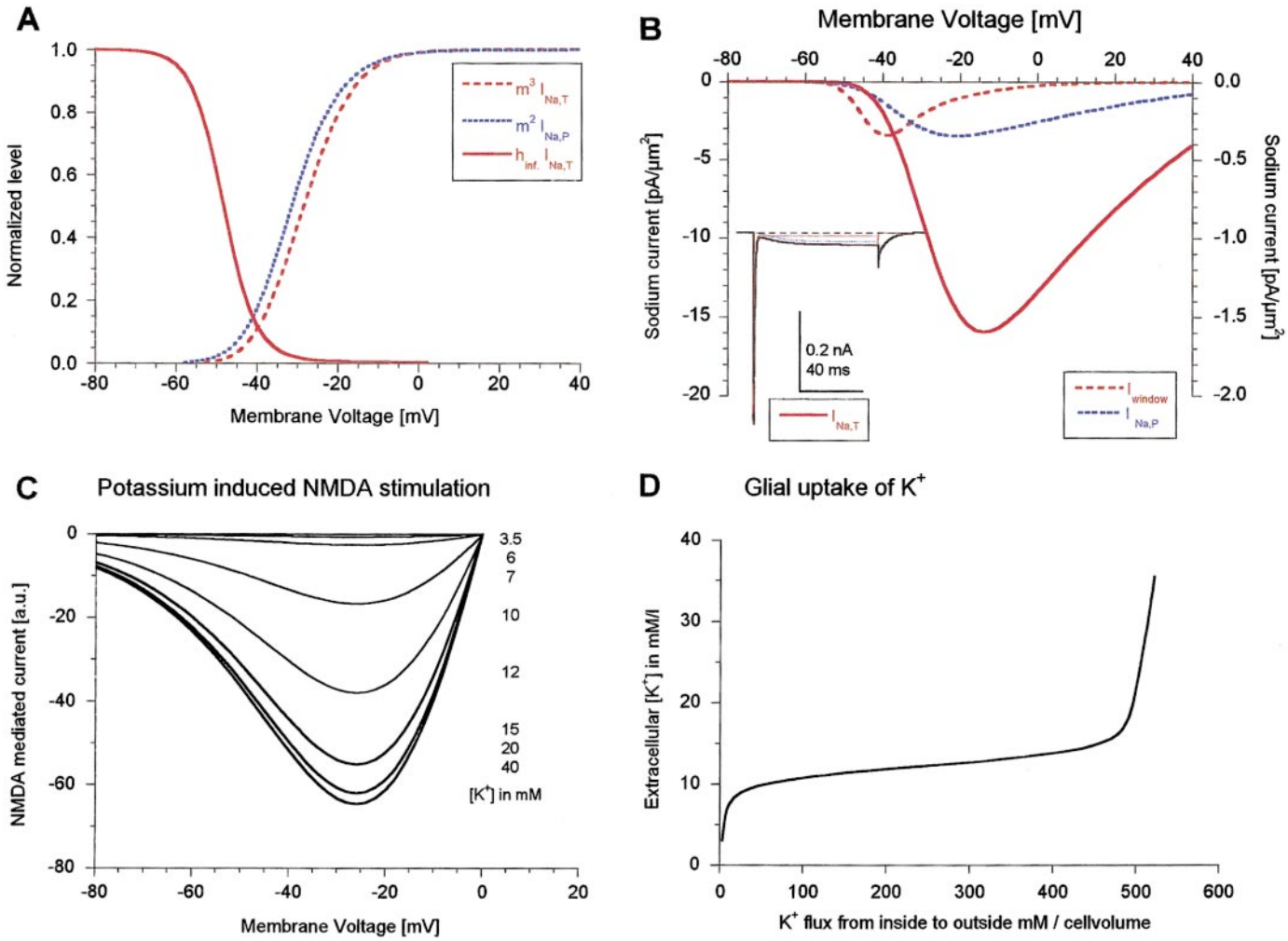

FIG. 2. Properties of some of the simulated currents. *A*: activation and inactivation functions: $m^3\ I_{Na,T}$: activation of the transient Na^+ current; $m^2\ I_{Na,P}$: activation of the persistent Na^+ current; h_{inf}: steady-state inactivation of the transient Na^+ current. Note that the curves for h_{inf} and m^3 overlap, creating a voltage domain or "window" where $I_{Na,T}$ is partially activated but inactivation is as yet incomplete. *B*: current-voltage (*I-V*) curves of the transient and persistent sodium currents and the window current of $I_{Na,T}$. The *left ordinate axis* refers to $I_{Na,T}$, the *right axis* to $I_{Na,P}$ and the "window" current. *Inset*: $I_{Na,T}$, $I_{Na,P}$, and their sum, evoked by depolarizing step from −90 to −20 mV. (note the window current as continued flow of $I_{Na,T}$). *C*: *I-V* curves of the glutamate-induced *N*-methyl-D-aspartate (NMDA) current that is dependent on voltage (through Mg^{2+} block) as well as, indirectly, on extracellular potassium (concentrations indicated at right side of figure). *D*: properties of the glial potassium buffering system. Abscissa: flux of K^+ out of the neuron; ordinate: extracellular potassium concentration resulting from the flux. Channel currents and pump current were ignored for this illustration. The kinetics of the buffering were fast enough to assume virtually instantaneous equilibrium.

in a neuron soma. Figure 2*B* (*inset*) shows the transient and persistent sodium currents, $I_{Na,T}$ and $I_{Na,P}$ and their sum, evoked by a voltage step from −90 to −10 mV. Similarly to "real life" whole cell recordings, repolarization elicited an inward tail current due to the slow closing of the $I_{Na,P}$ channels. In Fig. 2*A*, the activation and steady-state inactivation (m^3 and h) curves are plotted. Of note is the presence of a window current between the membrane potentials of −50 and 20 mV, in which region activation begins but steady-state inactivation is not yet complete (see also Magee and Johnston 1995; Sah et al. 1988). This enables $I_{Na,T}$ to flow continuously, influencing the behavior of the model in depolarized states. In Fig. 2*B*, *inset*, the window current is visible as the continued flow of $I_{Na,T}$ beyond the termination of the main current surge. Its importance will become clear in the results.

Persistent Na current, $I_{Na,P}$

A persistent sodium current was inserted into the somatic and the dendritic compartments. The voltage dependence and kinetics that describe this sodium current were mainly based on data obtained from hippocampal preparations. In dissociated hippocampal CA1 neurons $I_{Na,P}$ activates between −60 and −70 mV, and it is maximal between −20 and −40 mV in different cells (Somjen, unpublished data, similar to those published by French et al. 1990; Hammarström and Gauge 1998).

We used a kinetic scheme (see also Fig. 2, *A* and *B*)

$$I_{Na,P} = g_{Na,P} * m^2 * h * \mathrm{GHK}(Na_i, Na_o, V)$$

The value for the maximal conductance, $g_{Na,P}$ was taken to be much smaller than the one for $g_{Na,T}$ and equal to $2 * 10^{-5}$ S/cm^2. Because little information is available about the activation kinetics we simplified it to

$$\alpha_m = m_\infty/\tau_{activation} \quad \text{and} \quad \beta_m = (1 - m_\infty)/\tau_{activation}$$

with

$$\tau_{activation} = 6 \text{ ms} \quad \text{and} \quad m_\infty = \frac{1}{1 + \exp - (0.143 * V + 5.67)}$$

Downloaded from www.physiology.org/journal/jn by ${individualUser.givenNames} ${individualUser.surname} (129.034.020.019) on December 28, 2017.
Copyright © 2000 American Physiological Society. All rights reserved.

Inactivation is extremely slow (10^6 times slower than that of $I_{Na,T}$), and it was modeled similar to the fast transient Na current giving

$$\alpha_h = 5.12 * 10^{-8} * \exp - (0.056 * V + 2.94)$$

and

$$\beta_h = \frac{1.6 * 10^{-6}}{1 + \exp - (0.2 * V + 8)}$$

Delayed rectifier K current $I_{K,DR}$

The noninactivating potassium current was inserted in all compartments and obeyed the kinetic scheme of

$$I_{K,DR} = g_{K,DR} * n^2 * \mathrm{GHK}(K_i, K_o, V)$$

Using a density for $g_{K,DR}$ of $100 * 10^{-5}$ S/cm^2 and the following voltage dependent rate constants

$$\alpha_n = 0.016 * \frac{-V - 34.9}{\exp -(0.2 * V + 6.98) - 1}$$

and

$$\beta_n = 0.25 * \exp - (0.025 * V + 1.25)$$

Transient K current $I_{K,A}$

The fast transient potassium current I_A was implemented in all compartments with a kinetic scheme that obeyed

$$I_{K,A} = g_{K,A} * m^2 * h * \mathrm{GHK}(K_i, K_o, V)$$

and a value of $g_{K,A}$ of $10 * 10^{-5}$ S/cm^2. The activation kinetics was implemented as

$$\alpha_m = 0.02 * \frac{-V - 56.9}{\exp - (0.1 * V + 5.69) - 1}$$

and

$$\beta_m = 0.0175 * \frac{V + 29.9}{\exp(0.1 * V + 2.99) - 1}$$

and for the inactivation gate

$$\alpha_h = 0.016 * \exp - (0.056 * V + 4.61)$$

and

$$\beta_h = \frac{0.5}{1 + \exp - (0.2 * V + 11.98)}$$

NMDA receptor mediated current, I_{NMDA}

We reasoned that global glutamate-dependent depolarization can be modeled as NMDA receptor activation. Since there is evidence that glutamate is released from cells when $[K^+]_o$ is elevated (Crowder et al. 1987; Fujikawa et al. 1996) and high $[K^+]_o$ also enhances NMDA receptor activation (Poolos and Kocsis 1990), the conductance, g_{NMDA}, was made a function of $[K^+]_o$ as well as of voltage (Hestrin et al. 1990) (see Fig. 2*C*). Given the long-lasting phenomena that we study and the fast desensitization rate of the AMPA receptor, we concentrated our efforts on depolarizations mediated by the NMDA receptor. It was only inserted in the dendritic compartments and was implemented including its voltage-dependent Mg^{2+} block (Traub et al. 1994). The current was carried by both, Na^+ and K^+, giving it an apparent reversal potential around -10 mV (Fig. 2*C*)

$$I_{Na} = g_{NMDA} * m * h * \frac{\mathrm{GHK}(Na_i, Na_o, V)}{1 + 0.33 * [Mg^{2+}]_0 * \exp - (0.07 * V + 0.7)}$$

which is apart from the driving force equal to

$$I_K = g_{NMDA} * m * h * \frac{\mathrm{GHK}(K_i, K_o, V)}{1 + 0.33 * [Mg^{2+}]_0 * \exp - (0.07 * V + 0.7)}$$

with $[Mg^{2+}]_0$ set to 1.2 mM/l and g_{NMDA} equal to $10 * 10^{-5}$ S/cm^2.

The kinetics of the receptor consisted of a fixed activation time constant of 2 ms and a fixed desensitization of 2,000 ms so that we get for the activation

$$\alpha_m = m_\infty / \tau_{\mathrm{activation}}$$

with

$$\tau_{\mathrm{activation}} = 2 \text{ ms} \quad \text{and} \quad m_\infty = \frac{1}{1 + \exp\left(\frac{\mathrm{Kha} - [K]_0}{\mathrm{Ksa}}\right)}$$

where Kha is 13.5 mM/l and Ksa is 1.42 mM/l, and for desensitization

$$\alpha_h = h_\infty / \tau_{\mathrm{desensitization}}$$

with

$$\tau_{\mathrm{desensitization}} = 2000 \text{ ms and } h_\infty = \frac{1}{1 + \exp\left(\frac{[K]_0 - \mathrm{Khi}}{\mathrm{Ksi}}\right)}$$

where Khi is 6.75 mM/l and Ksi is 0.71 mM/l.

Ion accumulation

In our model, the membrane currents are carried by ions, and this has been taken into account as an actual change in ion concentration. This made it necessary to define an extracellular space as the interstitial volume fraction, ISVF, which was taken to be a fixed fraction of the intracellular space (15%) based on published data (see DISCUSSION) (Mazel et al. 1998; McBain et al. 1990). For simplicity, we did not calculate the lateral diffusion between adjacent compartments.

All transmembrane sodium and potassium currents were integrated and converted into chemical units to continuously calculate intra- and extracellular ion concentrations. In all compartments instantaneous diffusion equilibrium was assumed

$$\frac{\mathrm{d}[\mathrm{Ion}]_i}{\mathrm{d}t} = \frac{I_{\Sigma(\mathrm{Ion})} * \mathrm{Surface}}{F * \mathrm{Vol}_{\mathrm{intra}}}$$

where F is the Faraday constant, Surface is the surface area related to the ion densities included, and $\mathrm{Vol}_{\mathrm{intra}}$ is the intracellular volume of the compartment under study. Since the ions have to flow into the accompanying extracellular compartment they also change the concentration there

$$\frac{\mathrm{d}[\mathrm{Ion}]_o}{\mathrm{d}t} = -\frac{I_{\Sigma(\mathrm{Ion})} * \mathrm{Surface}}{F * \mathrm{Vol}_{\mathrm{extra}}}$$

where we assume a fixed relation between the intracellular volume and the interstitial space

$$\mathrm{Vol}_{\mathrm{extra}} = \mathrm{ISVF} * \mathrm{Vol}_{\mathrm{intra}} \quad \text{with} \quad \mathrm{ISVF} = 0.15$$

(see also DISCUSSION). "Resting" ion concentrations were set to (in mM/l): $[Na^+]_o$, 130; $[Na^+]_i$, 10; $[K^+]_o$, 3; $[K^+]_i$, 130.

Active pumping of Na and K ions

An essential feature of our model is the accumulation and depletion of ions in the intra- and extracellular space (see following text). To balance these effects, we implemented an active pump that was able to restore the balance for sodium and potassium ions. It is stimulated by extracellular $[K^+]$ and intracellular $[Na^+]$. We assume instantaneous kinetics, which, however, due to the integrating nature of the ion concentrations, will always be slow. The pump will contribute an electrogenic factor because it exchanges 2 K^+ for 3 Na^+. Its rate is

Downloaded from www.physiology.org/journal/jn by ${individualUser.givenNames} ${individualUser.surname} (129.034.020.019) on December 28, 2017.
Copyright © 2000 American Physiological Society. All rights reserved.

determined by the concentrations according to the following relation (Läuger 1991)

$$A_{pump} = \left(1 + \frac{Km_K}{[K^+]_o}\right)^{-2} * \left(1 + \frac{Km_{Na}}{[Na^+]_i}\right)^{-3}$$

using Km_K of 3.5 mM/l and Km_{Na} of 10 mM/l, contributing to the ion flux with

$$I_K = -2 * I_{max} * A_{pump}$$

$$I_{Na} = 3 * I_{max} * A_{pump}$$

The maximal flux (converted to electrical units), I_{max}, generated by the pump was adjusted to obtain a steady state under resting conditions just compensation the ion leaks. The usual value of I_{max} was 0.013 mA/cm^2.

Control of extracellular K accumulation

Potassium accumulation in the interstitial volume was controlled by a first-order buffering scheme that simulated an effective glial potassium uptake system. It had a fixed backward rate constant (k_1) and a forward rate constant (k_2) that was potassium dependent. In an extracellular volume fraction of 15% of the intracellular volume, the total capacity of the potassium buffer was set to have a concentration of 500 mM

$$[K^+] + [Buffer] \underset{\Leftarrow k_1}{\overset{\Rightarrow k_2}{}} [Kbuffer]$$

with rate constants

$$k_1 = 0.0008$$

and

$$k_2 = \frac{0.0008}{1 + \exp\left(\frac{K^+ - 15}{-1.09}\right)}$$

where $[K^+]$ is the potassium concentration in the interstitial space, and [Buffer] and [Kbuffer] are, respectively, the lumped free and bound buffer in the same volume. This function describes extracellular buffering phenomenologically. The speed of the buffering was dependent on the extracellular K^+ concentration, but despite the relative low rate constants, it appeared in all situations that we encountered to achieve a virtually instantaneous equilibrium. The kinetic aspects of the K^+ buffering system were not investigated in further detail. In Fig. 2*D* we illustrate this properties by plotting the final K^+ concentration that is reached in the extracellular space when a certain amount of K^+ is entered, assuming in this figure that no other mechanisms are present. At low concentrations relatively little K^+ is buffered, but at around 10 mM/l the buffer capacity is quite high, creating a relative ceiling corresponding to the so-called "ceiling" of $[K^+]_o$ (Heinemann and Lux 1977). It takes a large amount of K^+ before the buffer is saturated and thereafter fast increase can occur again, ultimately raising K^+ up to levels where the driving force becomes the limiting factor (around 30–60 mM/l). We have limited our model calculations by ignoring diffusion of K^+ (and other ions) among the compartments of the extracellular space. This probably exaggerates the duration of extracellular ionic gradients in comparison with the real situation, although lateral diffusion through the limited interstitial volume will be unimportant compared with diffusion/uptake at locations farther away from the cell membrane.

Numerical considerations

The actual simulation and numerical integration was performed in NEURON using a higher-order variable time step integration procedure (Hines and Carnevale 1997). The model was numerically stable. In many situations, we repeated the simulation with a forced smaller time step to check whether numerical stability or accuracy was affecting the results. The most important aspect was calculation of the membrane voltage in the extended dendritic tree treated with cable equations (further described by Hines and Carnevale 1997). An additional but essential complication was that we also simulated the effects of ionic currents on extra- and intracellular ion concentrations. Under conditions of the repetitive firing, seizures and SD large ionic shifts occur that have to be taken into account when driving forces for the ionic currents are calculated. They were therefore continuously evaluated using the accumulated ion concentrations. Local diffusion in the neighborhood of ionic channels or flux limitations through the channels were not taken into account.

By adjusting the densities of the leaks and fine tuning the "pump," the resting potential was initially always set to near −70 mV. Cell impedance and membrane time constant were kept within the physiological range. When intracellular stimulation was performed, we mimicked the experimental situation with a sharp electrode in the somatic compartment that allowed the injection of current, ignoring possible shunt effects. Input impedance was determined through the same current injection configuration, by injecting a small hyperpolarizing current pulse and measuring the resulting voltage step.

RESULTS

"Resting" properties and normal excitability of the model

With the initial ion concentrations set to $[K^+]_o/[K^+]_i$ = 3.5/133.5 and $[Na^+]_o/[Na^+]_i$ = 140/10, the equilibrium potentials of these two ions was at "rest" E_K = −97 mV and E_{Na} = +71 mV. Before starting a trial, the leak conductances and the pump maximal turnover rate were set to achieve at the soma a stable membrane potential, V_m, stable ion concentrations and input resistance, R_{in}, conforming to experimental data. Thus the resting V_m was between −69 and −71 mV in different trials, and, in the absence of stimulation, it did not change by more than 0.5–1 mV in 80 s of simulated time. The resting R_{in} varied between 40 and 105 MΩ in different simulations, in the great majority between 40 and 60 MΩ, values well within the range measured with "sharp" electrodes in CA1 pyramidal neurons (Müller and Somjen 1998, 2000; Schwartzkroin and Mueller 1987).

The response of the model neuron to stimulation when $[K^+]_o$ was well controlled is illustrated in Fig. 3. A depolarizing current of 0.1 nA was applied for 200 ms to the cell soma. As long as the current flowed, the model generated a series of action potentials that stopped shortly after cessation of the pulse. At first each action potential was followed by a hyperpolarizing afterpotential, generated by the voltage-gated potassium conductances $g_{K,A}$ and $g_{K,DR}$. During each action potential, the cell lost K^+ to the extracellular fluid and gained Na^+ at the expense of $[Na^+]_o$, resulting in step-wise shifts of E_K and E_{Na}. After several spikes, E_K reached the "foot" of the spikes so that there was no more driving force remaining for the generation of the afterhyperpolarizations, and eventually V_m was forced to a more positive level in the interspike intervals. The disappearance of the hyperpolarizing afterpotential under the influence of K^+ accumulating in interstitial space is akin to the Frankenhaeuser-Hodgkin effect seen during repetitive stimulation of the squid giant axon (Frankenhaeuser and Hodgkin 1956). After termination of the stimulating current, V_m briefly dipped below E_K, forced into hyperpolarization by the electrogenic Na-K ion pump, which was strongly activated by the

Downloaded from www.physiology.org/journal/jn by ${individualUser.givenNames} ${individualUser.surname} (129.034.020.019) on December 28, 2017.
Copyright © 2000 American Physiological Society. All rights reserved.

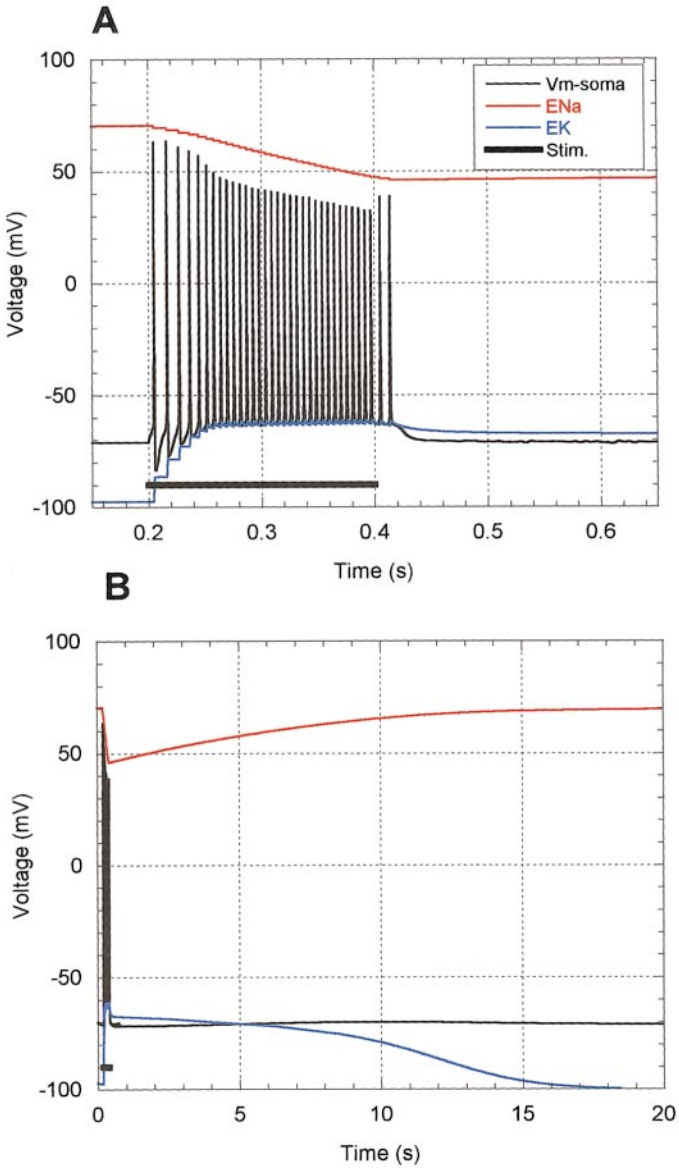

FIG. 3. The normal response of the model in its stable state. The tracings were obtained from the "soma" segment of the model neuron shown in Fig. 1. Black trace: the membrane potential (V_m); red line: the equilibrium potential computed for Na^+ (E_{Na}); blue line: the equilibrium for K^+ (E_K). The horizontal bar indicates the application of a 0.1-nA depolarizing pulse to the soma. *A* and *B* represent the same event on 2 different time scales.

rises in $[Na^+]_i$ and $[K^+]_o$. After the end of the stimulus-induced firing it took about 17 s for V_m, E_{Na}, and E_K to be restored to their resting values by the Na-K pump.

Afterdischarge and intermittent ("clonic") burst behavior

The behavior of the model changed dramatically when the maximal turnover capacity of the Na-K pump was weakened by 44%. In this state, when the same current pulse was applied to the soma as in Fig. 3, the spike train did not stop at the end of stimulus but continued for several hundreds of milliseconds (Fig. 4, *A* and *B*). Firing continued because the continued elevation of $[K^+]_o$ kept V_m depolarized above the threshold for firing. The firing stopped when $[Na^+]_i$ increased and $[Na^+]_o$ decreased so much that the declining electrochemical gradient for Na^+ and the lingering inactivation of g_{Na} raised the threshold for firing beyond reach. Thereafter the model continued to generate bursts of action potentials at regular intervals without any additional outside intervention (Fig. 4*C*). Following each burst, the electrogenic effect of the Na-K pump drove V_m more negative than E_K. The electrical load imposed on the soma by the dendrites (Fig. 4*D*) also aided hyperpolarization of the soma. In the absence of fast sodium channels, the dendrites did not generate action potentials of their own, but the electrotonic coupling with the soma produced the spikelets of the V_m tracing seen in Fig. 4*D* (see Fig. 1, for the location of dendritic segment d2). Because of the slow recovery of E_K, the membrane potential in the soma could not return to its rest level after completing a spike burst but began to slowly depolarize again. Since the pump current is a joint function of $[K^+]_o$ and of $[Na^+]_i$, as the ion levels shifted toward their normal value, the pump current gradually decreased. As the pump's action weakened, the control of V_m, was once more taken over by the leak currents, as shown by the crossing of V_m over E_K (Fig. 4*C*). Now because E_{Na} recovered faster than E_K, V_m was still depolarized. At this time, $g_{Na,T}$ inactivation had been sufficiently removed, and the driving force for I_{Na} was restored in order for another burst of action potentials to be triggered. So the cycle repeated itself.

SD-like depolarization

Figures 5–7 illustrate various features of one example of a simulated SD-like event. To generate this SD-like depolarization, $g_{Na,P}$ was increased in the entire neuron membrane. Furthermore the dendritic tree has been equipped with a conductance whose properties resemble those of NMDA receptor-controlled channels. To activate I_{NMDA}, it was assumed that NMDA receptor activation is enhanced and that glutamate is released into the interstitial space from glial cells and axon terminals whenever these structures are depolarized by rising $[K^+]_o$ (Crowder et al. 1987; Fujikawa et al. 1996; Poolos and Kocsis 1990).

In the simulation of Fig. 5, a depolarizing current of 0.2 nA was applied for 0.5 s to the soma of the model. The cell fired at a high rate, and firing continued well beyond the end of the stimulation (Fig. 5*A*). During the afterdischarge, the firing frequency increased while the amplitude of the spikes decreased and the level of V_m in the inter-spike intervals became more and more positive. Slightly more than 0.5 s after the end of the stimulating pulse, the membrane settled into a depolarized and inactivated state. In the ensuing seconds, V_m continued to move from around −40 to about −20 mV and then started to repolarize slowly due to an ever reduced E_{Na} (Fig. 5*B*). During and after the depolarizing pulse, E_K rose and approached V_m, but it caught up with the latter only during the inactivated state. In other simulated SD-like depolarizations, E_K did not always come to equal V_m, but the two variables always approached and tended to move along parallel trajectories during the depolarization but suddenly parted company at the moment of V_m repolarization. How near V_m and E_K became during an SD-like event depended on the relative values chosen for ion conductances and pump turnover capacity. In the example of Fig. 5, approximately 25 s after the start of the trial, V_m suddenly repolarized and overshot to a hyperpolarized level and then it gradually returned toward its resting

Downloaded from www.physiology.org/journal/jn by ${individualUser.givenNames} ${individualUser.surname} (129.034.020.019) on December 28, 2017.
Copyright © 2000 American Physiological Society. All rights reserved.

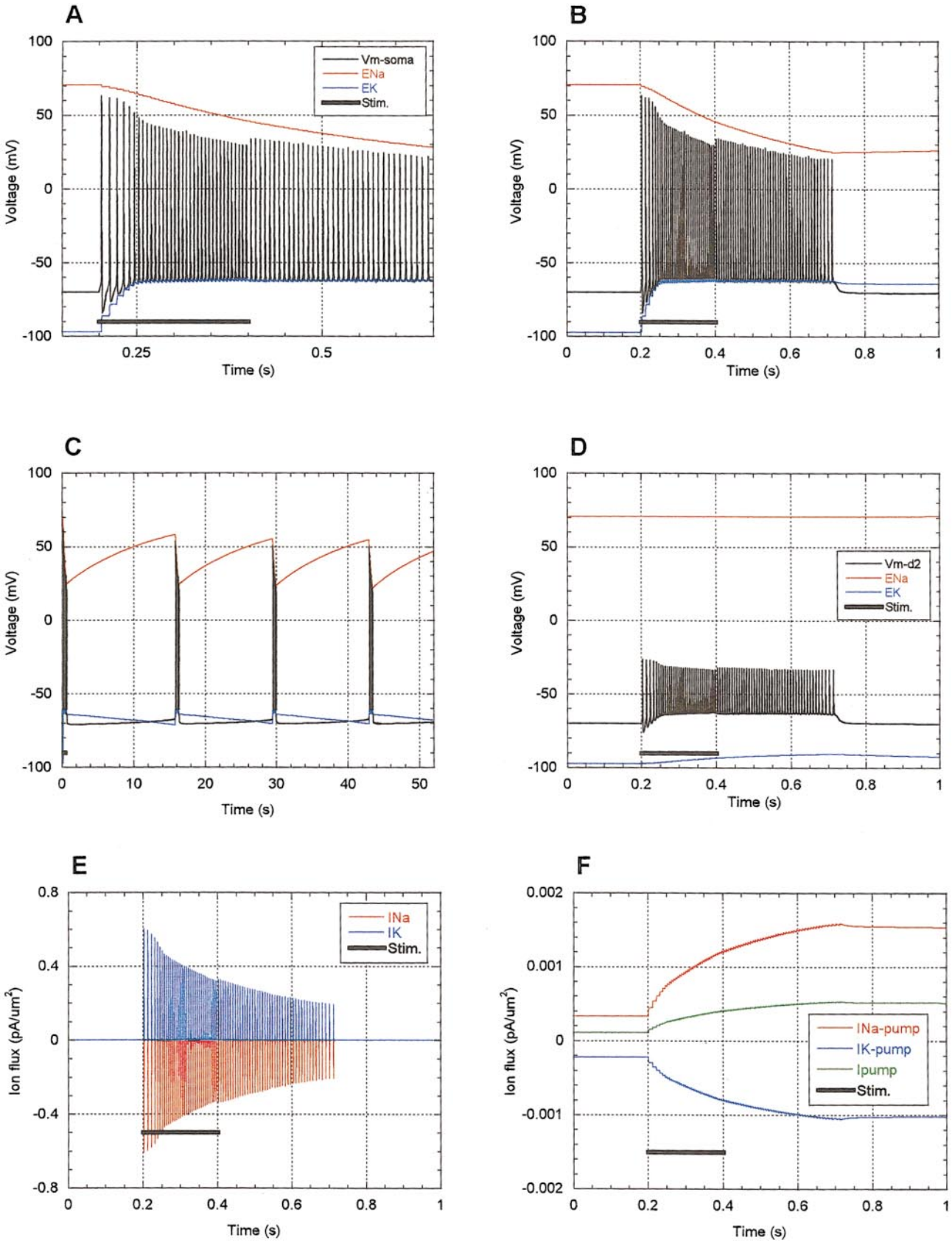

FIG. 4. Prolonged afterdischarge followed by recurrent (clonic) seizure discharges generated by the model neuron. The 6 panels show different aspects of the same event. In each graph, the horizontal bar indicates the single 0.1-nA depolarizing pulse applied to the soma at the beginning of the simulation. *A–C*: the membrane potential and the equilibrium potentials for Na^+ and K^+ in the cell soma, plotted on 3 different time scales. *D*: the same 3 variables in the proximal dendrites (dendritic segment 2, see Fig. 1). *E*: sodium and potassium currents recorded in the soma. *F*: transport of Na^+ (red line) and of K^+ (blue line) in the soma by the Na-K exchange pump, expressed in electric units ($pA/\mu m^2$). The green line represents the net pump current, which is electrogenic.

Downloaded from www.physiology.org/journal/jn by ${individualUser.givenNames} ${individualUser.surname} (129.034.020.019) on December 28, 2017.
Copyright © 2000 American Physiological Society. All rights reserved.

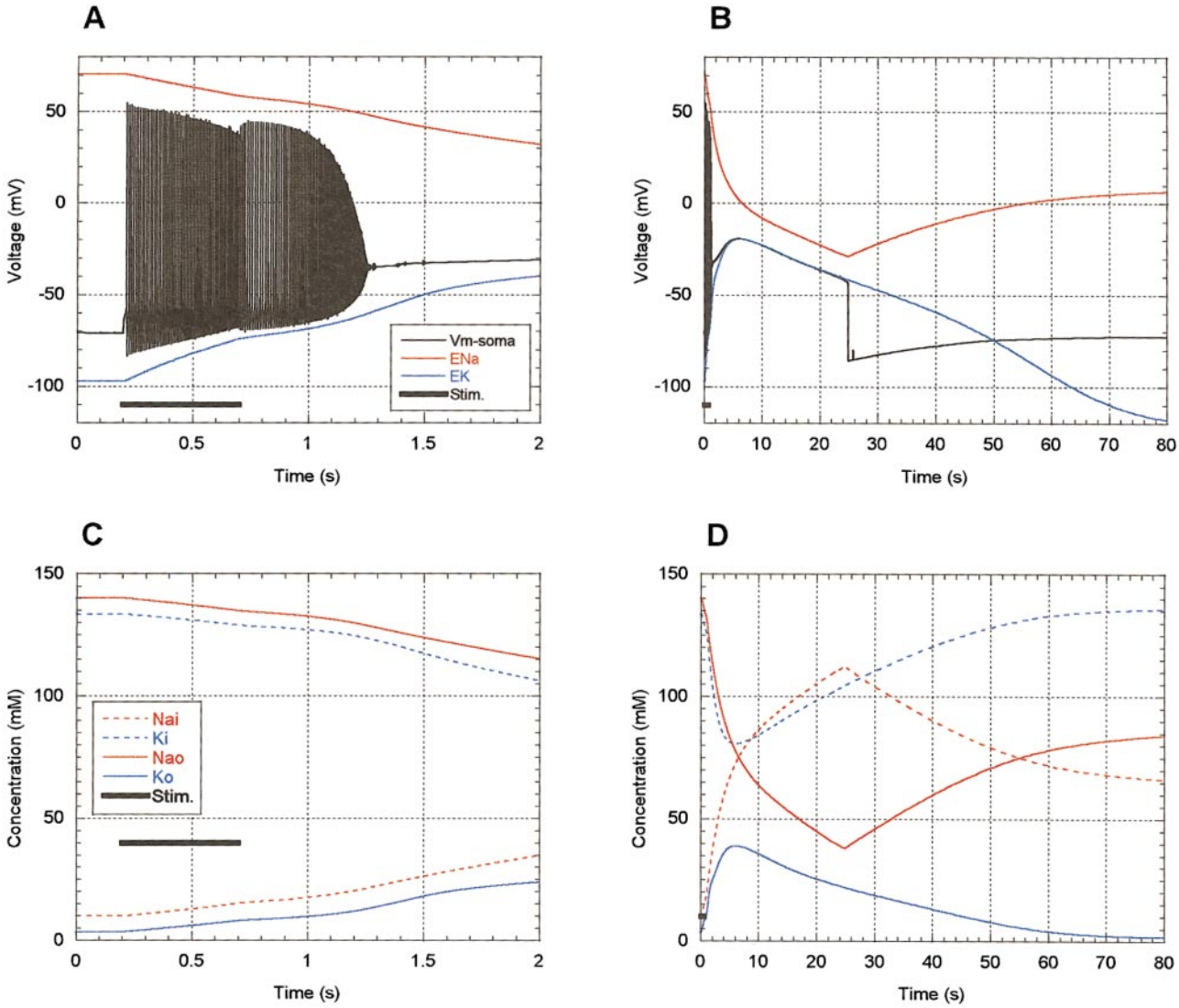

FIG. 5. Seizure discharge followed by spreading depression (SD)-like depolarization, recorded in the cell soma. All 4 panels derived from the cell soma during the same event. The horizontal bars represent a depolarizing pulse of 0.2 nA, 500 ms, applied to the cell soma. *A* and *B*: V_m, E_{Na}, and E_K represented similarly to Figs. 3 and 4, *A–C*. *C* and *D*: the changes in concentrations of Na^+ and K^+ in the interstitial space and in cytosol ($[Na^+]_o$ and $[K^+]_o$, respectively, $[Na^+]_i$ and $[K^+]_i$).

voltage, while E_K now slowly descended to eventually reach a level considerably more negative than at rest (Fig. 5*B*). Undershoots of voltage and $[K^+]_o$ are well-known features of tracings of SD in live brain tissue (Hansen and Zeuthen 1981; Heinemann and Lux 1975).

The changes in ion concentrations are illustrated in Fig. 5, *C* and *D*. These were computed assuming that ISVF is 15% of cell volume (for a critique see DISCUSSION). $[K^+]_o$ rose to almost 30 mM during the SD-like depolarization, which is well within the range seen in experiments. $[Na^+]_o$ dipped to about 30 mM, which is lower than usual in real life but not excessively so. Hansen and Zeuthen (1981) reported an average of 60 mM, Kraig and Nicholson (1978) reported 57 mM during SD, and we found recently 61 ± 16 (StD) mM during hypoxic SD-like depolarization (Müller and Somjen, 2000). $[K^+]_o$ started to recover already during the depolarized phase, but $[Na^+]_o$ continued to decrease and $[Na^+]_i$ to increase while the depolarized state lasted due to the continued flow of Na^+ current (Fig. 7, *A* and *B*). In this period, the slowly inactivating voltage-gated conductances $g_{Na,P}$ and $g_{K,DR}$ were both high, but while Na^+ ions were still experiencing a considerable driving force, there remained no driving force for K^+ ions. Figure 6, *A* and *B*, illustrates the courses of V_m, E_{Na}, and E_K in the proximal dendrites (Fig. 1, dendrite 2) during the same trial as Fig. 5. As before, only attenuated, electrotonically conducted spikelets were recorded here because no $I_{Na,T}$ existed in this segment (Fig. 6*A*). After a short delay following the spike discharge, V_m in the dendrites depolarized rapidly to a short-lived summit, and then it began to repolarize slowly (Fig. 6*B*). Abrupt hyperpolarization occurred in the dendrites at the same time as in the soma. The time courses of V_m in the soma and in the proximal and distal dendrites are compared in Fig. 6, *C* and *D*. A delay of 0.28 s between the steep depolarizations of distal and proximal dendrites is evident in Fig. 6*A*. With the distance between the two segments being 238 μm, this works out to an apparent propagation velocity of 0.84 μm/ms. The initial courses of V_m in the dendritic segments d2 and d14 are remarkably similar, suggesting all-or-none type responses that

Downloaded from www.physiology.org/journal/jn by ${individualUser.givenNames} ${individualUser.surname} (129.034.020.019) on December 28, 2017.
Copyright © 2000 American Physiological Society. All rights reserved.

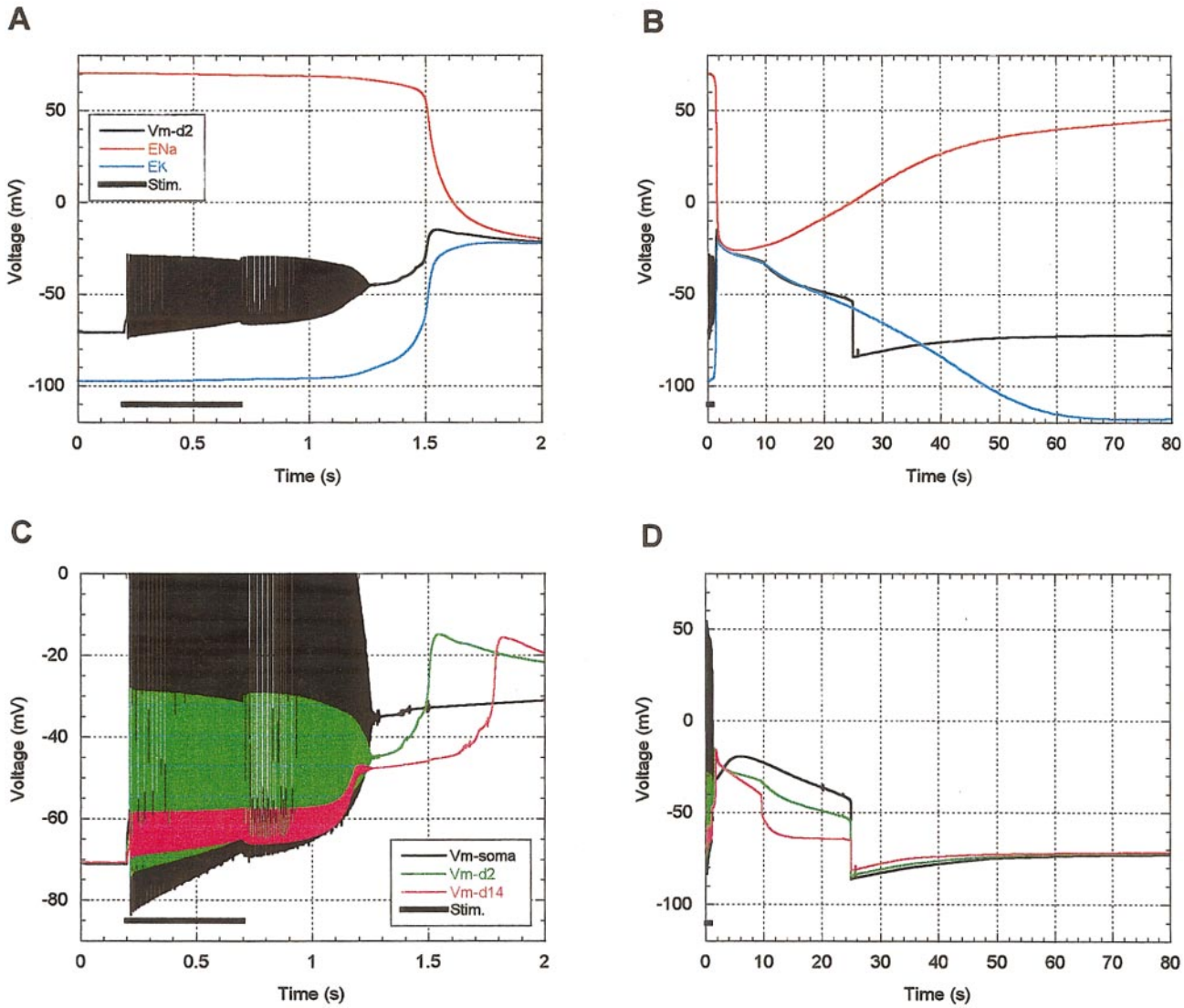

FIG. 6. Voltages recorded in different segments of the model neuron during the same SD-like event as in Fig. 5. *A* and *B*: V_m, E_{Na}, and E_K in the proximal dendrites (d2), on 2 different time scales. *C* and *D*: superimposed tracings of the membrane potentials recorded in soma, in proximal, and in distal dendrites (d2 and d14).

were propagated slowly along the dendrites. V_m in segment d14 repolarized in two steps, the first one after about 10 s, probably due to the activity of the d14 segment's membrane itself, while the second hyperpolarizing effect was apparently imposed on this segment electrotonically from its "upstream" neighbors. Similar discontinuities have been seen in other SD simulations.

Figure 7 illustrates the currents that generated the voltages shown in Figs. 5 and 6. Following the burst of action potentials, V_m remained depolarized in the soma by the combined effect of the window current of $I_{Na,T}$ plus the activation of $I_{Na,P}$ (Fig. 7, *A* and *B*). The window current subsided as V_m depolarized into the voltage range where inactivation (h) became more effective (Fig. 5*A*), and then it increased again somewhat as V_m repolarized into the range where the window is most open (Fig. 7*B*; compare also Fig. 2, *A* and *B*). Thus $I_{Na,P}$ and the window of $I_{Na,T}$ were taking turns in keeping the membrane depolarized, and their joint action was shaping the course of V_m. The window closed suddenly when V_m repolarized beyond -50 mV. Even though both currents, $I_{Na,P}$ and the window current, are small, they could keep the membrane depolarized because of the minimal opposition by I_K, which was minimal in the absence of an electrochemical gradient for K^+ ions. In fact, for a short while I_K was flowing inward instead of outward, reversing course ever so slightly, (Fig. 7*B*). In other successful simulations of SD, such a reversal did not always occur, and it is therefore not a requirement for the generation of SD. In such cases, it was enough if the outwardly directed I_K became small.

In the dendrites, the sustained SD-like depolarization was the result of cooperative activation of $I_{Na,P}$ and I_{NMDA} (Fig. 7, *C* and *D*). $I_{Na,P}$ was activated first, due to the initial depolarization conducted electrotonically from the soma. Then I_{NMDA} followed when $[K^+]_o$ began to rise. A positive feedback evolved as I_{NMDA} released K^+ ions raising $[K^+]_o$, which then reinforced I_{NMDA} so that its increase accelerated, driving V_m in the dendrites to a depolarized summit well before the soma (compare Figs. 7*C* and 6, *C* and *D*). Rapid change in dendrites is also aided by the greater surface to volume ratio. After reaching its peak, I_{NMDA} subsided due to the desensitization of

Downloaded from www.physiology.org/journal/jn by ${individualUser.givenNames} ${individualUser.surname} (129.034.020.019) on December 28, 2017.
Copyright © 2000 American Physiological Society. All rights reserved.

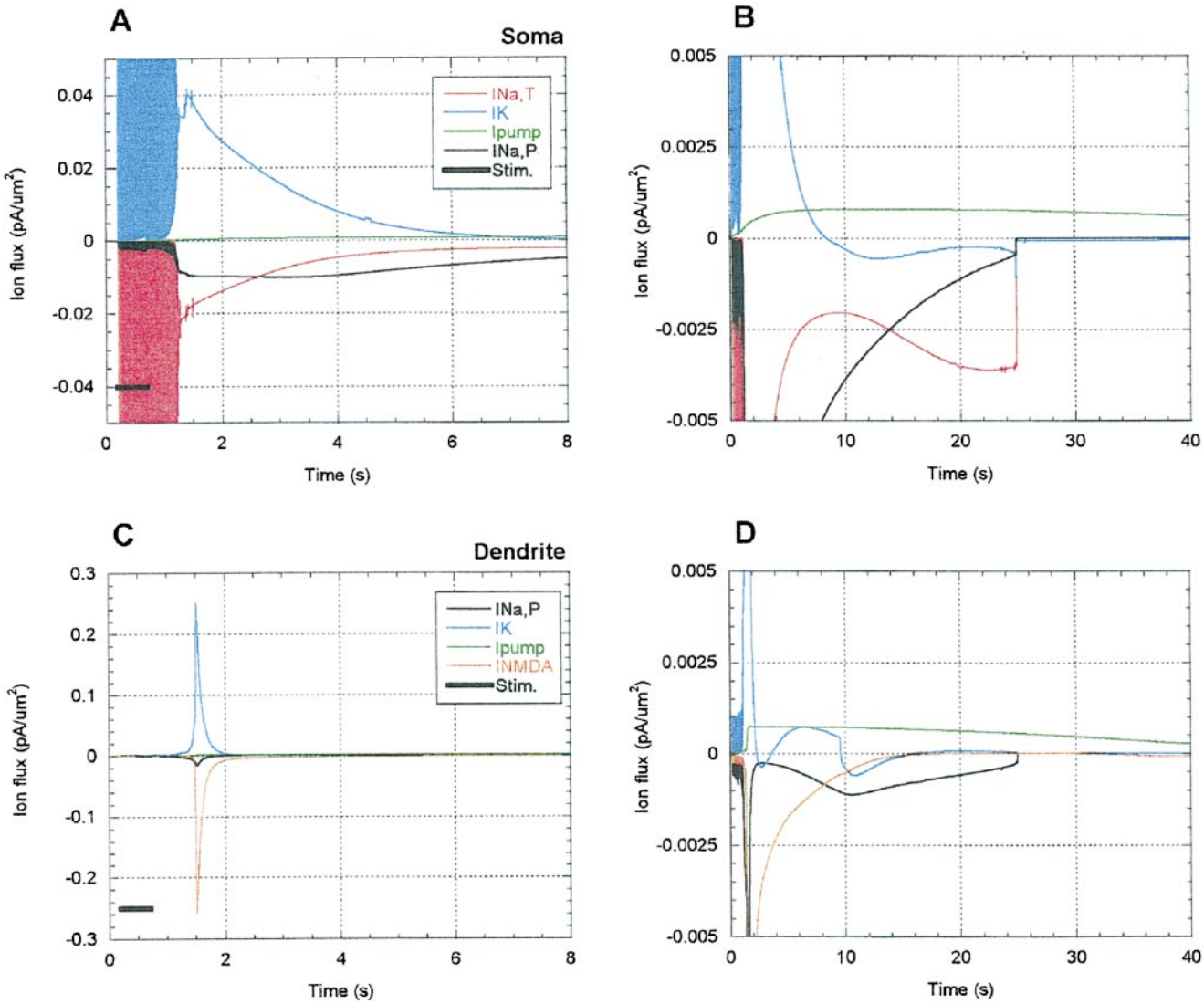

FIG. 7. Ion currents recorded during the same SD-like event as Figs. 5 and 6. *A* and *B*: the transient and persistent sodium currents ($I_{Na,T}$ and $I_{Na,P}$), the total potassium current ($I_{K,DR}+I_{K,A}$) and the net pump current in the soma, plotted on 2 different sets of abscissal and ordinal scales. *C* and *D*: similar tracings for the proximal dendrites, d2. I_{NMDA} represents the NMDA receptor-controlled current.

the receptor. Meanwhile, however, $I_{Na,P}$ has increased sufficiently to maintain depolarization (Fig. 7*D*).

During most of the SD-like event the only force opposing depolarization was the net pump current, and it was the pump current alone that hyperpolarized the cell after the collapse of the inward currents (Fig. 7, *B* and *D*). It may be surprising that the very small net outward pump current could generate the very large and sudden hyperpolarizing shift. This was possible because of the rebounding membrane resistance, which suddenly became high once all active ion channels had shut down. The input resistance of the soma of the model of Fig. 7 was 50 MΩ at rest, it dropped to 0.67 MΩ at the peak of the depolarization and shortly after cessation of impulse firing. At the end of the depolarized phase it was 6.6 MΩ and during the maximally hyperpolarized state again 51 MΩ. SD was produced in numerous simulations under varying conditions. While the details varied, the essential features were similar in all cases.

Critical ignition point of the SD process

The tracings of Fig. 8 were produced by the model in the same state as for Figs. 5–7 except that the threshold at which the glial uptake function began to operate was set at 8 mM $[K^+]_o$ for Fig. 8, while it was 10 mM for the simulation of Fig. 5–7. With the glial uptake starting at a lower level, $[K^+]_o$ could not rise above 7.9 mM during the fixed period of stimulation (Fig. 8*B*). With $[K^+]_o$ remaining at a low ceiling, the conditions for maintained depolarization and afterdischarge were absent, $I_{Na,P}$, the $I_{Na,T}$ window current, and I_{NMDA} were not activated. The stimulating current induced repetitive firing but no afterdischarge, and the SD-like all-or-none response was not triggered (Fig. 8*A*).

Component actors of the SD-like process

The simulation illustrated in Figs. 5–7 was produced by the cooperation of a number of currents. We asked whether fewer

Downloaded from www.physiology.org/journal/jn by ${individualUser.givenNames} ${individualUser.surname} (129.034.020.019) on December 28, 2017.
Copyright © 2000 American Physiological Society. All rights reserved.

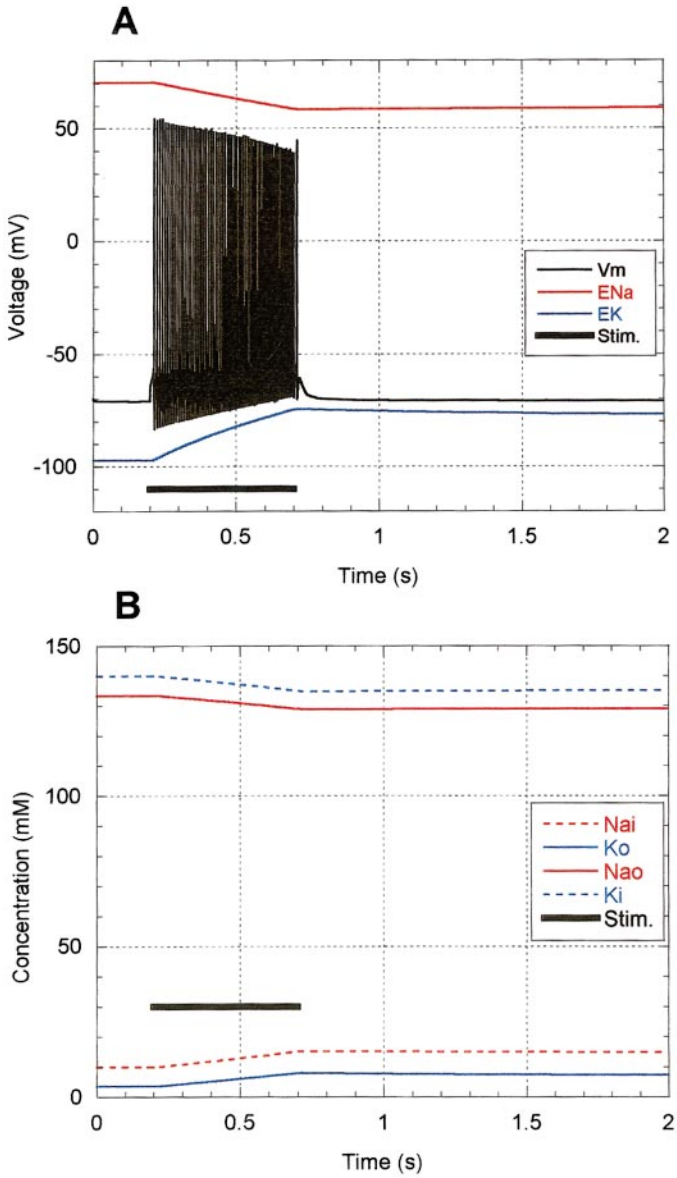

FIG. 8. Restoration of a stable state. All the parameters as well as the stimulating current were the same as for the SD-like event of Figs. 5–7, except that the threshold for the "glial uptake" function was lowered from 10 to 8 mM $[K^+]_o$. Compare especially the traces of $[K^+]_o$ in *B* of with Fig. 5*C*.

of these currents could produce an SD-like response. In the simulation shown in Fig. 9 $I_{Na,P}$ and both K currents were inserted in soma and dendrites, but $I_{Na,T}$ and I_{NMDA} were absent. Stimulation by a depolarizing current of 0.3 nA for 0.5 s produced an SD-like response in soma as well as in the dendrites (Fig. 9, *A–C*). As shown in Fig. 9*B*, the time delay among the three compartments was quite short. Depolarization began in the soma, the site of the stimulating current (Fig. 9*B*), but the summit of depolarization was reached first in the distal dendrites followed by the proximal dendrites and finally in the soma (Fig. 9*C*). The maximal amplitude of the depolarization was, however, largest in the soma, smaller in the proximal dendrites, and smaller yet distally (Fig. 9*C*) even though the initial courses of V_m were very similar (Fig. 9*B*). As also seen in the case of Fig. 6*D*, in Fig. 9*C*, in the distal dendrites, V_m repolarized before the other segments, and then it was pulled into hyperpolarization by the neighboring segments several seconds later. In this case, the input resistance at rest was 43 MΩ, at the height of depolarization, it dropped to 0.96 MΩ, toward the end of the SD-like event it was 4.1 MΩ, and immediately after repolarization, in the hyperpolarized state it was 46 MΩ.

Figure 10 illustrates a trial in which the cell soma was endowed only with $I_{K,DR}$ and $I_{K,A}$, while the dendritic tree had the two K currents and also an NMDA receptor-controlled current. The soma was depolarized by a 2-nA current for 2 s. As expected, there was no active response to this very strong stimulus in the soma, yet the dendrites did generate an SD-like response (Fig. 10, *A–D*). When there was an "active" SD-process in the soma (Figs. 5–7 and 9), it tended to prolong the depolarization of the dendrites. In the absence of SD in the soma, the dendrites repolarized in less than 8 s (Fig. 10*B*). The cell soma, which had no inward current, was nevertheless forced to remain partially depolarized by electrotonus by the dendritic response (Fig. 10, *A* and *B*). The courses of V_m in three of the model's compartments are compared in Fig. 10*A*. The shape of the curve depicting V_m in the distal dendrite (d14) is almost identical to that in the proximal dendrite (d2), but it is delayed by almost 1 s (Fig. 10, *A* and *B*). The propagation velocity in this case was only 0.28 μm/ms, again suggesting an all-or-none type response propagating along the cable structures of the dendritic tree.

Other pathophysiological behaviors of the model

When $I_{Na,T}$ and the two K currents were in place in the soma, but $I_{Na,P}$ was small, I_{NMDA} was absent, and the Na-K pump and "K-uptake" functions were set at low capacity, strong depolarizing pulses often produced high-frequency firing that ended in a partially depolarized and inactivated state either already during the flow of stimulating current or following a few seconds of afterdischarge. In these cases, the membrane potential seemed fixed between −35 and −50 mV, within the window of the $g_{Na,T}$. Eventually the cell started to repolarize, and, as it did so, it sometimes resumed firing for a short period before returning to its resting state. This sequence resembled intracellular recordings sometimes obtained from neurons during tonic seizures (e.g., Fig. 10 of Somjen et al. 1985).

In a simulated cell soma without dendrites, surrounded by the usual interstitial space and endowed with the Hodgkin-Huxley style conductances but no $I_{Na,P}$ or I_{NMDA}, strong stimuli provoked repetitive firing at a constant frequency that could indefinitely outlast the stimulating pulse. The continuous firing was maintained by elevated $[K^+]_o$, which fluctuated with each spike around a stable mean level. We mention this behavior for the sake of completeness even though it has no equivalent counterpart in real life.

DISCUSSION

The results of these simulations warrant several general conclusions. First is that single neurons are capable of producing the self-sustaining pathophysiological processes typical of at least some types of epileptiform seizures as well as those of Leão's SD. Second is that there is no need to postulate novel membrane conductances but rather that these processes can be generated by the abnormal activity of "physiological" ion

Downloaded from www.physiology.org/journal/jn by ${individualUser.givenNames} ${individualUser.surname} (129.034.020.019) on December 28, 2017.
Copyright © 2000 American Physiological Society. All rights reserved.

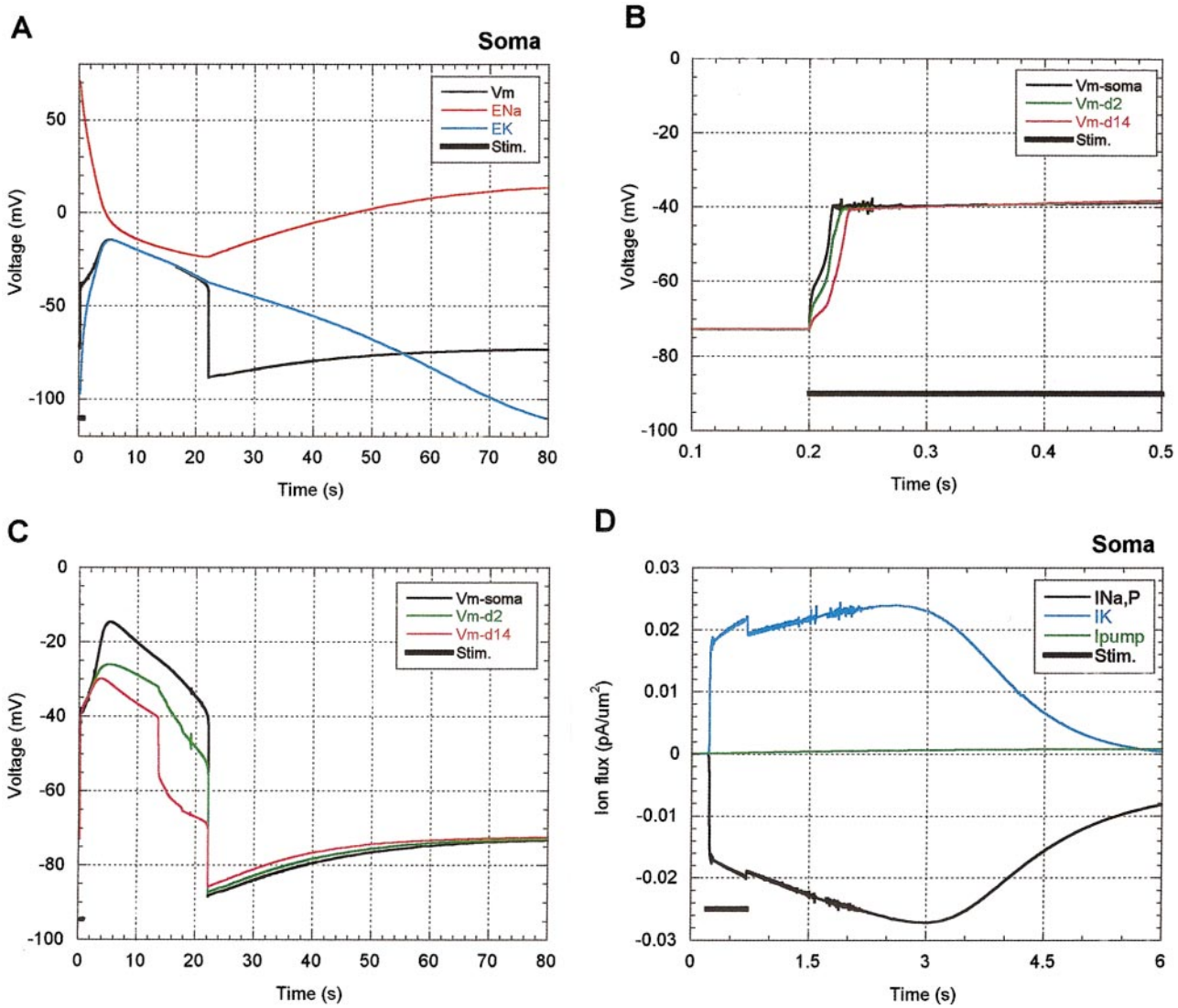

FIG. 9. SD-like depolarization can be produced when the persistent sodium current is the only inward current. For this simulation, $I_{Na,T}$ and I_{NMDA} have been deleted. The stimulus was 0.3 nA for 500 ms. *A*: membrane potential and ion equilibrium potentials recorded in the cell soma. *B* and *C*: membrane voltages in three segments of the model neuron superimposed on different time scales. *D*: the persistent sodium current, the summed potassium currents, and the net pump current recorded in the cell soma.

channels. Third, the key to the generation of prolonged seizure discharge and SD is the positive feedback based on ion currents causing ion concentration changes, and ion concentration changes altering ion currents. And, as a corollary, is that the normal stability of brain function rests on the ability of cerebral tissue to keep ion distributions within well-regulated limits.

It follows, that the ability to generate self-sustaining inward current is not specific to any single ion channel type. To produce such a current, a channel must have the following properties: it must conduct inward current, it must be either voltage or $[K^+]_o$ dependent (or both), and the inward current must (secondarily) induce the release of K^+ ions into a restricted extracellular space. A seizure will erupt if the membrane potential is forced to remain above firing threshold but below inactivation level. SD-like suspended excitability requires an inward current with inactivation (or desensitization) that is slow or absent. SD will result if the membrane potential moves into the range where the spike-generating currents are inactivated.

The basic idea is not new. Years ago Grafstein (1956) proposed a potassium hypothesis for SD and Hodgkin used diffusion theory to show how the movement of K^+ in interstitial space could explain the propagation of SD; Hodgkin's unpublished derivation was incorporated in a communication by Grafstein (1963). Later Green (1964) and Fertziger and Ranck (1970) proposed that positive feedback mediated by elevated $[K^+]_o$ had a key role in the initiation and maintenance of epileptiform seizures. As an alternative to Grafstein's (1956) potassium hypothesis, Van Harreveld and Fifková (1970) proposed that the agent of positive feedback is glutamate. Like K^+ ions, glutamate is released from cells during SD and it can induce SD. Later Van Harreveld modified his position and proposed a dual hypothesis in which both K^+ and glutamate play a part (Van Harreveld 1978). The limited knowledge of the biophysics of central neurons and the absence of computational techniques prevented critical testing of these early propositions at the time of their publication. Our simulations lend credence to Van Harreveld's dual hypothesis.

Downloaded from www.physiology.org/journal/jn by ${individualUser.givenNames} ${individualUser.surname} (129.034.020.019) on December 28, 2017.
Copyright © 2000 American Physiological Society. All rights reserved.

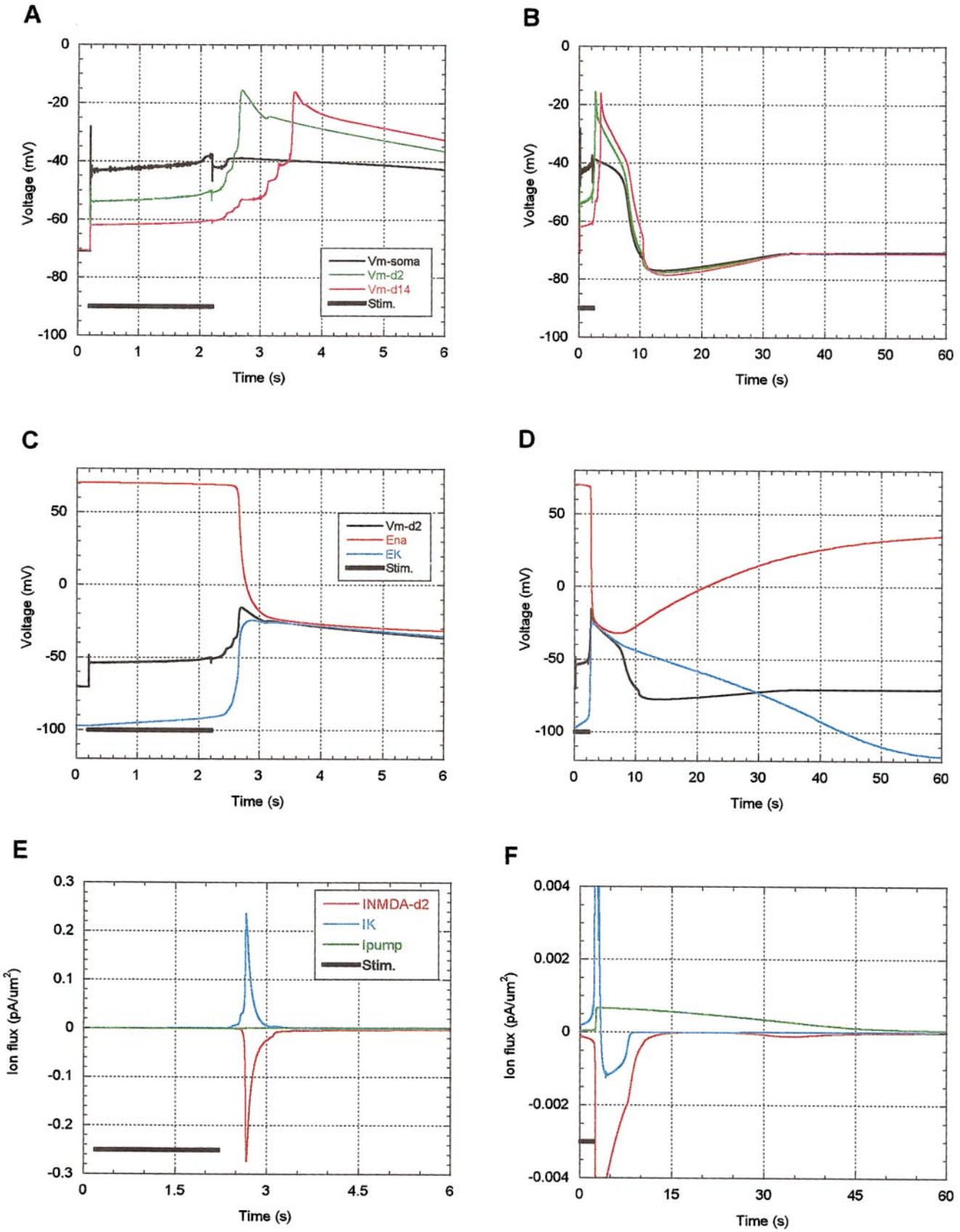

FIG. 10. SD-like depolarization generated in the dendrites by NMDA receptor-controlled current ($I_{Na,P}$) by itself. $I_{Na,T}$ and $I_{Na,P}$ have been deleted. The stimulus was 2 nA applied for 2 s. *A* and *B*: the membrane potentials in 3 cell segments superimposed on 2 different time scales. *C* and *D*: membrane potential and ion equilibrium potentials in the proximal dendritic segments (d2). *E* and *F*: ion currents in the proximal dendritic segments (d2).

Downloaded from www.physiology.org/journal/jn by ${individualUser.givenNames} ${individualUser.surname} (129.034.020.019) on December 28, 2017.
Copyright © 2000 American Physiological Society. All rights reserved.

It has been known for some time that drugs blocking either glutamate-controlled or voltage-gated Na currents can delay and curtail but not prevent SD and SD-like hypoxic depolarization (Hernández-Cáceres et al. 1987; Herreras and Somjen 1993a,b; Marrannes et al. 1988). More recently we found that a pharmacological cocktail inhibiting all known major voltage-gated and receptor-controlled Na^+ and Ca^{2+} currents succeeds in suppressing hypoxic SD where individual ingredients of the cocktail failed (Müller and Somjen 1998). In the model neuron, it was sufficient to have either a voltage-gated persistent Na conductance or an NMDA receptor-controlled conductance to generate the SD-like depolarization. In real life and in the absence of blocking drugs, glutamate-induced and voltage-gated inward currents probably cooperate in generating SD. This explains why blocking either the one or the other will reduce but not eliminate SD, while suppressing all inward currents simultaneously does succeed in preventing SD. More recently M. Müller and G. G. Somjen (unpublished data) tested whether blocking glutamate receptors and voltage-gated Na^+ currents, but leaving Ca^{2+} currents active, prevents hypoxic SD in hippocampal slices. In this condition, withdrawing oxygen still provoked SD in three of six slices and in five of eight pyramidal neurons, albeit only after an unusually long delay and at a greatly elevated threshold level of $[K^+]_o$. On the other hand, replacing all but 25 mM of the Na^+ in the bathing solution by *N*-methyl-D-glucamine ($NMDG^+$) completely but reversibly prevented the occurrence of hypoxic SD even though none of the membrane channels was blocked, indicating that Ca^{2+} alone cannot mediate SD. It follows that, besides the glutamate- and voltage-controlled channels, there is some additional pathway for Na^+ influx that can mediate SD-like depolarization even if in blunted form. A possible candidate may be the acetylcholine and Ca^{2+} dependent cation current described by Fraser and MacVicar (1996) (see also Kawasaki et al. 1999).

The potassium hypothesis of seizure generation proposed by Fertziger and Ranck (1970) was disputed by Heinemann et al. (1978), who could not find a fixed threshold of $[K^+]_o$ at which seizures would erupt. Yet they emphasized that once a seizure started, elevated $[K^+]_o$ could shape its progress. Recently Borck and Jefferys (1999) proposed that elevated $[K^+]_o$ causes the transition from interictal to ictal discharge. In the simulations presented here, seizures had to be triggered by a depolarizing stimulating current; elevated $[K^+]_o$ maintained the discharge, it did not start it. Seizures could be provoked by the initial stimulus provided that the regulation of $[K^+]_o$ was less than optimal. This role of high $[K^+]_o$ in the simulation is entirely compatible with the observed behavior of $[K^+]_o$ during seizures (Fertziger and Ranck 1970; Heinemann et al. 1978; Somjen and Giacchino 1985). Also in agreement with measurements in live brain tissue are the membrane hyperpolarization and the undershoot of $[K^+]_o$ below its rest level, mediated in the simulations by the Na-K pump after the termination of seizure discharges and of SD-like depolarization (Heinemann and Gutnick 1979; Heinemann et al. 1978). These authors already emphasized the role of electrogenic ion transport in the termination of seizure discharges. In our simulations, postexcitation undershoot of the membrane potential preceded the recovery and undershoot of potassium levels both in the "normal" state (Fig. 3) and in the inter-burst intervals during seizures (Fig. 4, *B* and *C*). As a result, for short periods, V_m was more negative than E_K. There are no published simultaneous measurements of K^+ concentrations and neuron membrane potentials during seizures in live brain tissue to verify this feature, but extracellular recordings are compatible with it because following spike trains, seizures or SD, V_o returns to baseline or undershoots baseline well before $[K^+]_o$ does (Borck and Jefferys 1999; Hansen and Lauritzen 1984; Heinemann and Gutnick 1979; Heinemann and Lux 1975; Heinemann et al. 1978; Nicholson 1984; Somjen and Aitken 1984; Somjen and Giacchino 1985).

While computer simulations cannot positively prove a point, they can decide whether a theoretical explanation of a process is feasible and consistent (for a detailed discussion, see Borg-Graham 1999). The model presented here had many but by no means all the properties of a real neuron. Epileptic attacks do, of course, require an intact organism whose brain, muscles, and viscera produce the clinical picture. Single neurons are, however, the constituent units of the system, and understanding their properties is essential for understanding the operation of the organism. Our model did not produce a complete tonic-clonic seizure sequence only prolonged afterdischarges followed by unceasingly recurring "clonic" discharges. It may be that *grand mal* attacks can only be generated by cell populations connected in a network of excitatory and inhibitory connections. Moreover these simulations cannot speak to the mechanism by which SD or Jacksonian seizures propagate only to the mechanism by which these processes evolve once they have been ignited. The propagation velocities estimated from dendritic recordings (Figs. 6*C* and 10*A*) are by far faster than the 2–5 mm/min with which SD spreads in the brain. In the model neuron, the SD wave was conducted along the dendritic cables, while the customary measurements in brain tissue concern movement from cell to cell, and this cannot be imitated in a model consisting of a single neuron.

Other, earlier computer simulations interpreted the propagation of SD in terms of a diffusion-reaction process but did not address the specific membrane currents generating the depolarization (Grafstein 1963; Tuckwell and Miura 1978). Reggia and Montgomery (1996) and Revett et al. (1998) attempted to relate simplified theoretical models of SD to the pathophysiology of clinical conditions. In a recent abstract, Shapiro (1999) outlined a model testing the role of gap junctions in the propagation of SD.

In our model, the SD-like depolarization evolved faster in the dendrites than in the soma. In an analysis of high K^+-induced SD in rat hippocampus in situ, the extracellular voltage shifts (ΔV_o) almost always started in stratum radiatum before st. pyramidale (Herreras and Somjen 1993b). The typical, biphasic, "inverted saddle" shape of the ΔV_o suggested at least two mechanisms contributing to the process. This impression was reinforced when the NMDA antagonist compound CPP apparently blocked the second, larger component of the dual-peaked ΔV_o. The analysis of multiple recordings of ΔV_o (Herreras and Somjen 1993a,b) and the simulations presented here are compatible with the idea of at least two generators of the SD process, only one of which is NMDA dependent.

The geometry of the model was that of a real neuron, as published in the Duke-Southampton Archive of Neuronal Morphology (Cannon et al. 1998) with values for membrane capacitance and cytoplasmic resistivity conforming to known physiological parameters (see METHODS). The input conduc-

Downloaded from www.physiology.org/journal/jn by ${individualUser.givenNames} ${individualUser.surname} (129.034.020.019) on December 28, 2017.
Copyright © 2000 American Physiological Society. All rights reserved.

tance of cells was within the range encountered in CA1 pyramidal neurons in real life (e.g., Brown et al. 1981; Fujimura et al. 1997; Fujiwara et al. 1987; Müller and Somjen 1998, 2000; Schwartzkroin and Mueller 1987). The input conductances dropped during the height of SD to low values, as expected from published recordings (Czéh et al. 1993; Müller and Somjen 1998, 2000; Snow et al. 1983). The changes in ion concentrations and voltages that evolved during these simulations were also within the range of those measured in live brain tissue (Hansen and Zeuthen 1981; Kraig and Nicholson 1978; Müller and Somjen 2000). The all-or-none character of the simulated SD-like depolarization is similar to real SD. The ignition point for SD appears to have been reached when $[K^+]_o$ exceeded 8 mM (Figs. 8*B* and 5*C*), close to the 9 mM $[K^+]_o$ at which hypoxic SD-like depolarization took off in hippocampal slices (Müller and Somjen 2000).

While the behavior of the model was in many respects life-like, it did not emulate all aspects of real neurons. The differences can be ascribed to the numerous features that were missing from the model. The only Na^+ conductance in the dendrites of the model was the $g_{Na,P}$. There is much evidence for the existence of fast or intermediately inactivating Na^+ channels in dendritic membranes (Magee and Johnston 1995). These could play a role in initiating pathological discharges, but they do not seem to be essential for the process. Perhaps more important is the absence of calcium currents. Leaving calcium from our computations for the sake of simplicity was justified because seizure-like events and SD are known to occur in brain slices bathed in low-calcium solutions (Albrecht and Heinemann 1989; Basarsky et al. 1998, 1999; Dudek et al. 1990; Young and Somjen 1992). Glutamate is released into interstitial space during SD and other pathological conditions by both Ca-dependent and -independent processes (Basarsky et al. 1999; Benveniste et al. 1984; Drejer et al. 1985; Szerb 1991; Van Harreveld and Fifková 1970). Nonetheless, Ca currents and calcium-dependent K currents undoubtedly do modulate real seizures and SD. For example, the firing frequency of the model during simulated seizures was unusually high probably because of the absence of $I_{K(Ca)}$, which contributes to the slow hyperpolarizing afterpotentials. Another important omission from the model is the absence of chloride and of other anions. According to Nicholson (1984), the cerebellar cortex generates SD only if "conditioned", and one of the methods of conditioning is to replace Cl^- in the extracellular fluid by certain other anions. In isolated chick retina, Do Carmo and Martins-Ferreira (1984) found that replacing Cl^- by isethionate depressed the V_o shift associated with SD. Recently Müller (2000) confirmed this for hypoxic SD in hippocampal tissue slices using methylsulfate as the Cl^- substitute. Intracellular recording from neurons revealed, however, that while hypoxic SD-like depolarization of neurons was greatly delayed when $[Cl^-]_o$ was lowered, the ultimate level of the depolarization was not changed. It therefore appears that Cl^- flux modulates SD but is not an essential ingredient for its generation. A further omission from the model was any consideration given to charge balance.

Also missing, yet important, is the effect of cell swelling. Cells swell during seizures and during SD and SD-like hypoxic depolarization (Dietzel and Heinemann 1986; Hansen and Olsen 1980; Jing et al. 1994; Pérez-Pinzón et al. 1995), restricting interstitial space and hence amplifying extracellular ion concentration changes. The size of the interstitial space chosen for the simulation, 15% of the cell volume, was close to the 12–13% of the total tissue volume reported by McBain et al. (1990). A larger figure, about 20%, was recently suggested by Mazel et al. (1998). During SD, however, the interstitial volume fraction shrinks to around 5% (Jing et al. 1994). In an earlier and much simpler version of the model that consisted of a cell soma with sparsely branched apical dendrites, interstitial space was made to vary inversely and cell volume to vary directly with Na^+ uptake. The result was a dramatic decrease of the interstitial space during simulated SD. Restriction of interstitial space amplifies extracellular concentration changes and therefore accelerates the evolution of SD but does not qualitatively alter the process. Cell swelling probably participates in SD in yet another way by causing the release of glutamate through stretch-activated anion channels (Basarsky et al. 1999). Since elevated K^+ causes swelling, this is one more pathway cooperating in the positive feedback.

Another deficiency was the absence of lateral diffusion. Thus even though cell "compartments" were electrically coupled, for the computation of ion fluxes each was treated in isolation from its neighbors. Ion diffusion would smooth the sudden transitions in space and time. The next improvement of the model should take into account cell swelling as well as the missing ions, Ca^{2+} and Cl^-, charge balance, and spatial diffusion. These considerations will increase the complexity of computation by an order of magnitude. In the model, the distributions of K^+ and Na^+ were controlled by the Na-K pump. Conforming to its known properties (Läuger 1991), the pump transported three Na^+ ions against two K^+ ions. In addition, increases in $[K^+]_o$ were also limited by a glial uptake. The glial buffer hypothesis has appeared in the literature in several versions, but none is quantitative (reviewed by Somjen 1987). We represented the glial uptake in the form of a buffer without implying that it necessarily represents the actual mechanism. In intact brain, extracellular ion concentrations are also regulated by capillary endothelium that is capable of transporting not only K^+ but also Na^+ ions as well as other solutes between interstitial fluid and capillary blood.

French et al. (1990) first reported the existence of a persistent Na^+ current in dissociated hippocampal neurons. Mittmann et al. (1997) confirmed its presence in the dendritic tree of central neurons. It appears that $I_{Na,P}$ of hippocampal neurons is greatly enhanced during hypoxia (Hammarström and Gauge 1998). It has also been known since some time that raising $[K^+]_o$ had such an effect in skeletal and heart muscle (Barchi 1995; Hoffman et al. 1995). Enhancement of $I_{Na,P}$ by high $[K^+]_o$ has now been confirmed also in isolated hippocampal neurons (Somjen 2000) and in neurons in hippocampal slices (M. Müller and G. G. Somjen, unpublished results). More surprisingly, $I_{Na,P}$ was even more strongly potentiated when neurons filled with fluorescent calcium-indicator dyes were illuminated. These various methods of potentiating $I_{Na,P}$ may have a "final common path" that has yet to be discovered. The enhancement mediated by high $[K^+]_o$ and by hypoxia could amplify the positive feedback leading to SD and to hypoxic SD-like depolarization.

We conclude that seizure discharges and SD can be generated in healthy brain tissue if the normal regulatory mechanisms that keep ion concentrations within limits are overwhelmed. Spontaneous seizures, i.e., clinical epilepsy, can

Downloaded from www.physiology.org/journal/jn by ${individualUser.givenNames} ${individualUser.surname} (129.034.020.019) on December 28, 2017.
Copyright © 2000 American Physiological Society. All rights reserved.

result from inherently enhanced excitatory processes, defective synaptic inhibition, or failure of ion concentration regulation, three defects that could drive ion concentrations into the pathological range, and perhaps also from abnormal sensitivity (reduced threshold) of neurons to ion concentration change.

Finally we offer this speculation: could ordinary, everyday muscle cramp be the SD of skeletal muscle? Its sudden onset, all-or-none, autonomous, hard-to-influence course and its all too slow release are provocatively reminiscent of the course taken by SD of brain. Certainly potassium is abundantly available to serve as the agent of positive feedback in muscle and, as the cramp stops local blood flow, K^+ could accumulate in the interstitium.

This work was supported by National Institute of Neurological Disorders and Stroke Grant NS-18670.

REFERENCES

ALBRECHT D AND HEINEMANN U. Low calcium-induced epileptiform activity in hippocampal slices from infant rats. *Dev Brain Res* 48: 316–320, 1989.

BARCHI RL. Molecular pathology of the skeletal muscle sodium channel. *Annu Rev Physiol* 57: 355–385, 1995.

BASARSKY TA, DUFFY SN, ANDREW RD, AND MACVICAR BA. Imaging spreading depression and associates intracellular calcium waves in brain slices. *J Neurosci* 18: 7189–7199, 1998.

BASARSKY TA, FEIGHAN D, AND MACVICAR BA. Glutamate release through volume-activated channels during spreading depression. *J Neurosci* 19: 6439–6445, 1999.

BENVENISTE H, DREJER J, SCHOUSBOE A, AND DIEMER NH. Elevations of the extracellular concentrations of glutamate and aspartate in rat hippocampus during transient cerebral ischemia monitored by intracerebral microdialysis. *J Neurochem* 43: 1369–1374, 1984.

BORCK C AND JEFFERYS JGR. Seizure-like events in disinhibited ventral slices of adult rat hippocampus. *J Neurophysiol* 82: 2130–2142, 1999.

BORG-GRAHAM LJ. Interpretation of data and mechanisms for hippocampal pyramidal cell models. In: *Models of Cortical Circuits*, edited by Ulinski PS, Jones EG, and Peters A. New York: Plenum, 1999, p. 19–138.

BROWN TH, FRICKE RA, AND PERKEL DH. Passive electrical contansts in three classes of hippocampal neurons. *J Neurophysiol* 46: 812–827, 1981.

BUREŠ J., BUREŠOVÁ O, AND KŘIVÁNEK J. *The Mechanism and Applications of Leão's Spreading Depression of Electroencephalographic Activity.* Prague: Academia, 1974.

BUREŠ J., BUREŠOVÁ O, AND KŘIVÁNEK O. The meaning and significance of Leão's spreading depression. *An Acad Bras Cienc* 56: 385–400, 1984.

CANNON RC, TURNER DA, PYAPALI GK, AND WHEAL HV. An on-line archive of reconstructed hippocamnpal neurons. *J Neurosci Methods* 84: 49–54, 1998.

CROWDER JM, CROUCHER MJ, BRADFORD HF, AND COLLINS JF. Excitatory amino acid receptors and depolarization-induced Ca^{2+} influx into hippocampal slices. *J Neurochem* 48: 1917–1924, 1987.

CZÉH G, AITKEN PG, AND SOMJEN GG. Membrane currents in CA1 hippocampal cells during spreading depression (SD) and SD-like hypoxic depolarization. *Brain Res* 632: 195–208, 1993.

DIETZEL I AND HEINEMANN U. Dynamic variations of the brain cell microenvironment in relation to neuronal hyperactivity. *Ann NY Acad Sci* 481: 72–85, 1986.

DO CARMO RJ AND MARTINS-FERREIRA H. Spreading depression of Leao probed with ion-selective microelectrodes in isolated chick retina. *An Acad Bras Cienc* 56: 401–421, 1984.

DREJER J, BENVENISTE H, DIEMER NH, AND SCHOUSBOE A. Cellular origin of ischemia-induced glutamate release from brain tissue in vivo and in vitro. *J Neurochem* 45: 145–151, 1985.

DUDEK FE, OBENAUS A, AND TASKER JG. Osmolality-induced changes in extracellular volume alter epileptiform bursts independently of chemical synapses in the rat: importance of non-synaptic mechanisms in hippocampal epileptogenesis. *Neurosci Lett* 120: 267–270, 1990.

FERTZIGER AP AND RANCK JB. Potassium accumulation in interstitial space during epileptiform seizures. *Exp Neurol* 26: 571–585, 1970.

FRANKENHAEUSER B AND HODGKIN AL. The after-effects of impulses in the giant nerve fibers of Loligo. *J Physiol (Lond)* 131: 341–376, 1956.

FRASER DD AND MACVICAR BA. Cholinergic-dependent plateau potential in hippocampal CA1 pyramidal neurons. *J Neurosci* 16: 4113–4128, 1996.

FRENCH CR, SAH P, BUCKETT KJ, AND GAGE PW. A voltage-dependent persistent sodium current in mammalian hippocampal neurons. *J Gen Physiol* 95: 1139–1157, 1990.

FUJIKAWA DG, KIM JS, DANIELS AH, ALCARAZ AF, AND SOHN TB. In vivo elevation of extracellular potassium in the rat amygdala encreases extracellular glutamate and aspartate and damages neurons. *Neuroscience* 74: 695–706, 1996.

FUJIMURA N, TANAKA E, YAMAMOTO S, SHIGEMORI M, AND HIGASHI H. Contribution of ATP-sensitive potassium channels to hypoxic hyperpolarization in rat hippocampal CA1 neurons in vitro. *J Neurophysiol* 77: 378–385, 1997.

FUJIWARA N, HIGASHI H, SHIMOJI K, AND YOSHIMURA M. Effects of hypoxia on rat hippocampal neurones in vitro. *J Physiol (Lond)* 384: 131–151, 1987.

GLOOR P, SPERTI L, AND VERA CL. A consideration of feedback mechanisms in the genesis and maintenance of hippocampal seizure activity. *Epilepsia* 5: 213–238, 1964.

GLOOR P, VERA CL, SPERTI L, AND RAY SN. Investigation on the mechanism of epileptic discharge in the hippocampus. *Epilepsia* 2: 42–62, 1961.

GRAFSTEIN B. Mechanism of spreading cortical depression. *J Neurophysiol* 19: 154–171, 1956.

GRAFSTEIN B. Neuronal release of potassium during spreading depression. In: *Brain Function. Cortical Excitability and Steady Potentials*, edited by Brazier MAB. Berkeley, CA: University of California, 1963, p. 87–124.

GREEN JD. The hippocampus. *Physiol. Rev.* 44: 561–608, 1964.

HAMMARSTRÖM AKM AND GAGE PW. Inhibition of oxidative metabolism increases persistent sodium current in rat CA1 hippocampal neurons. *J Physiol (Lond)* 510: 735–741, 1998.

HANSEN AJ AND LAURITZEN M. The role of spreading depression in acute brain disorders. *An Acad Bras Cienc* 56: 457–480, 1984.

HANSEN AJ AND OLSEN CE. Brain extracellular space during spreading depression and ischemia. *Acta Physiol Scand* 108: 355–365, 1980.

HANSEN AJ AND ZEUTHEN T. Extracellular ion concentrations during spreading depression and ischemia in the rat brain cortex. *Acta Physiol Scand* 113: 437–445, 1981.

HEINEMANN U AND GUTNICK MJ. Relation between extracellular potassium concentration and neuronal activities in cat thalamus (VPL) during projection of cortical epileptiform discharge. *Electroencephalogr Clin Neurophysiol* 47: 345–347, 1979.

HEINEMANN U AND LUX HD. Undershoots following stimulus-induced rises of extracellular potassium concentration in cerebral cortex of cat. *Brain Res* 93: 63–76, 1975.

HEINEMANN U AND LUX HD. Ceiling of stimulus-induced rises in extracellular potassium concentration in the cerebral cortex of cats. *Brain Res* 120: 231–249, 1977.

HEINEMANN U, LUX HD, AND GUTNICK MJ. Changes in extracellular free calcium and potassium activity in the somatosensory cortex of cats. In: *Abnormal Neuronal Discharges*, edited by Chalazonitis N and Boisson M. New York: Raven, 1978, p. 329–345.

HERNÁNDEZ-CÁCERES J, MACIAS-GONZÁLEZ R, BROŽAEK G, AND BUREŠ J. Systemic ketamine blocks cortical spreading depression but does not delay the onset of terminal anoxic depression. *Brain Res* 437: 360–364, 1987.

HERRERAS O AND SOMJEN GG. Analysis of potential shifts associated with recurrent spreading depression and prolonged unstable SD induced by microdialysis of elevated K+ in hippocampus of anesthetized rats. *Brain Res* 610: 283–294, 1993a.

HERRERAS O AND SOMJEN GG. Propagation of spreading depression among dendrites and somata of the same cell population. *Brain Res* 610: 276–282, 1993b.

HESTRIN S, NICOLL RA, PERKEL DJ, AND SAH P. Analysis of excitatory synaptic action in pyramidal cells using whole-cell recording from rat hippocampal slices. *J Physiol (Lond)* 422: 203–225, 1990.

HILLE B. *Ionic Channels of Excitable Membranes.* Sunderland, MA: Sinauer, 1992.

HINES M AND CARNEVALE NT. The NEURON simulation environment. *Neural Computat* 9: 1179–1209, 1997.

HODGKIN AL AND HUXLEY AF. A quantitative description of membrane current and its application to conduction and excitation in nerve. *J Physiol (Lond)* 117: 500–544, 1952.

HOFFMAN EP, LEHMANN-HORN F, AND RÜDEL R. Overexcited or inactive: ion channels in muscle disease. *Cell* 80: 681–686, 1995.

Downloaded from www.physiology.org/journal/jn by ${individualUser.givenNames} ${individualUser.surname} (129.034.020.019) on December 28, 2017.
Copyright © 2000 American Physiological Society. All rights reserved.

JING J, AITKEN PG, AND SOMJEN GG. Interstitial volume changes during spreading depression (SD) and SD-like hypoxic depolarization in hippocampal tissue slices. *J Neurophysiol* 71: 2548–2551, 1994.

KAWASAKI H, PALMIERI C, AND AVOLI M. Muscarinic receptor activation induces depolarizing plateau potentials in bursting neurons of the rat subiculum. *J Neurophysiol* 82: 2590–2601, 1999.

KRAIG RP AND NICHOLSON C. Extracellular ionic variations during spreading depression. *Neuroscience* 3: 1045–1059, 1978.

LÄUGER P. *Electrogenic Ion Pumps.* Sunderland, MA: Sinauer, 1991.

LEÃO AAP. Spreading depression of activity in the cerebral cortex. *J Neurophysiol* 7: 359–390, 1944.

MAGEE JC AND JOHNSTON D. Characterization of single voltage-gated Na^+ and Ca^{2+} channels in apical dendrites of rat CA1 pyramidal neurons. *J Physiol (Lond)* 487: 67–90, 1995.

MARRANNES R, DE PRINS E, FRANSEN J, AND CLINCKE G. Neuropharmcology of spreading depression. In: *Migraine: Basic Mechanisms and Treatment*, edited by Lehmenkühler A, Grotemeyer K-H, and Tegtmeier F. Munich, Germany: Urban and Schwarzenberg, 1993, p. 431–443.

MARRANNES R, DE PRINS E, WILLEMS R, AND WAUQUIER A. NMDA antagonists inhibit cortical spreading depression, but accelerate the onset of neuronal depolarization induced by asphyxia. In: *Mechanisms of Cerebral Hypoxia and Stroke*, edited by Somjen G. New York: Plenum, 1988, p. 303–304.

MARSHALL WH. Spreading cortical depression of Leao. *Physiol Rev* 39: 239–279, 1959.

MAZEL T, SIMONOVÁ Z, AND SYKOVÁ E. Diffusion heterogeneity and anisotropy in rat hippocampus. *Neuroreport* 9: 1299–1304, 1998.

MCBAIN CJ, TRAYNELIS SF, AND DINGLEDINE R. Regional variation of extracellular space in hippocampus under physiological and pathological conditions. *Science* 249: 674–677, 1990.

MITTMANN T, LINTON SM, SCHWINDT P, AND CRILL W. Evidence for persistent Na+ current in apical dendrites of rat neocortical neurons from imaging of Na+-sensitive dye. *J Neurophysiol* 78: 1188–1192, 1997.

MÜLLER M. Effects of chloride transport inhibition and chloride substitution on neuron function and on hypoxic spreading depression-like depolarization in rat hippocampal slices. *Neuroscience* 97: 33–45, 2000.

MÜLLER M AND SOMJEN GG. Inhibition of major cationic inward currents prevents spreading depression-like hypoxic depolarization in rat hippocampal tissue slices. *Brain Res* 812: 1–13, 1998.

MÜLLER M AND SOMJEN GG. Na^+ and K^+ concentrations, extracellular and intracellular voltages and the effect of TTX in rat hippocampal slices during severe hypoxia. *J Neurophysiol* 83: 735–745, 2000.

NICHOLSON C. Comparative neurophysiology of spreading depression in the cerebellum. *An Acad Bras Cienc* 56: 481–494, 1984.

PÉREZ-PINZÓN MA, TAO L, AND NICHOLSON C. Extracellular potassium, volume fraction and tortuosity in rat hippocampal CA1, CA3 and cortical slices during ischemia. *J Neurophysiol* 74: 565–573, 1995.

POOLOS NP AND KOCSIS JD. Elevated extracellular potassium concentration enhances synaptic activation of N-mtheyl-D-aspartate receptors in hippocampus. *Brain Res* 508: 7–12, 1990.

PYAPALI GK, SIK A, PENTTONEN M, BUZSÁKI G, AND TURNER DA. Dendritic properties of hippocampal CA1 neurons in the rat: intracellular staining in vivo and in vitro. *J Comp Neurol* 391: 335–352, 1998.

RALL W, BURKE RE, HOLMES WR, JACK JJB, REDMAN SJ, AND SEGEV I. Matching dendritic neuron models to experimental data. *Physiol. Rev.* 72: S159–S186, 1992.

REGGIA JA AND MONTGOMERY D. A computational model of visual hallucinations in migraine. *Comput Biol Med* 26: 13–141, 1996.

REVETT K, RUPPIN E, GOODALL S, AND REGGIA JA. Spreading depression in focal ischemia: a computational study. *J Cereb Blood Flow Metab* 18: 998–1007, 1998.

SAH P, GIBB AJ, AND GAGE PW. The sodium current underlying action potentials in guinea pig hippocampal CA1 neurons. *J Gen Physiol* 91: 373–398, 1988.

SCHWARTZKROIN PA. Epileptogenesis in the immature central nervous system. In: *Electrophysiology of Epilepsy*, edited by Schwartzkroin PA and Wheal HV. London: Academic, 1984, p. 389–412.

SCHWARTZKROIN PA AND MUELLER AL. Electrophysiology of hippocampal neurons. *Cereb Cortex* 6: 295–343, 1987.

SHAPIRO BE. Leão's soreading depression and gap junctions: an electrodiffusion model of the voltage shift, ionic movement and osmotic volume changes. *Soc Neurosci Abstr* 25: 315, 1999.

SNOW RW, TAYLOR CP, AND DUDEK FE. Electrophysiological and optical changes in slices of rat hippocampus during spreading depression. *J Neurophysiol* 50: 561–572, 1983.

SOMJEN GG. Functions of glial cells in the cerebral cortex. *Cereb Cortex* 6: 1–39, 1987.

SOMJEN GG. Electrophysiology of mammalian glial cells in situ. In: *Neuroglial Cells*, edited by Kettenmann H and Ransom BR. Oxford, UK: Oxford Univ. Press, 1995, p. 319–331.

SOMJEN GG. Intracellular fluorescence and elevated $[K^+]_o$ potentiate persistent sodium current in isolated hippocampal neurons (Abstract). *FASEB J.* 14: A107, 2000.

SOMJEN GG AND AITKEN PG. The ionic and metabolic responses associated with neuronal depression of Leão's type in cerebral cortex and in hippocampal formation. *An Acad Bras Ciên* 56: 495–504, 1984.

SOMJEN GG, AITKEN PG, GIACCHINO JL, AND MCNAMARA JO. Sustained potential shifts and paroxysmal discharges in hippocampal formation. *J Neurophysiol* 53: 1079–1097, 1985.

SOMJEN GG, AITKEN PG, GIACCHINO JL, AND MCNAMARA JO. Interstitial ion concentrations and paroxysmal discharges in hippocampal formation and spinal cord. In: *Basic Mechanisms of the Epilepsies*, edited by Delgado-Escueta AV, Ward AA, Woodbury DM, and Porter RJ. New York: Raven, 1986, p. 663–680.

SOMJEN GG AND GIACCHINO JL. Potassium and calcium concentrations in interstitial fluid of hippocampal formation during paroxysmal responses. *J Neurophysiol* 53: 1098–1108, 1985.

SOMJEN GG, KAGER H, AND WADMAN WJ. Simulated seizures and spreading depression (Abstract). *2nd Meet Fed Eur Neurosci Soc*. In press.

SZERB JC. Glutamate release and spreading depression in the fascia dentata in response to microdialysis with high K+: role of glia. *Brain Res* 542: 259–265, 1991.

TRAUB RD, JEFFERYS JGR, MILES R, WHITTINGTON MA, AND TÓTH K. A branching dendritic model of a rodent CA3 pyramidal neurone. *J Physiol (Lond)* 481: 79–95, 1994.

TUCKWELL HC AND MIURA RM. A mathematical model for spreading cortical depression. *Biophys J* 23: 257–276, 1978.

VAN HARREVELD A. Two mechanisms for spreading depression in the chicken retina. *J Neurobiol* 9: 419–431, 1978.

VAN HARREVELD A AND FIFKOVÁ E. Glutamate release from the retina during spreading depression. *J Neurobiol* 2: 13–29, 1970.

VAN HARREVELD A AND STAMM JS. Spreading cortical convulsions and depressions. *J Neurophysiol* 16: 352–366, 1953.

VREUGDENHIL M, FAAS GC, AND WADMAN WJ. Sodium currents in isolated rat CA1 neurons after kindling epileptogenesis. *Neuroscience* 86: 99–107, 1998.

WADMAN WJ, JUTA AJA, KAMPHUIS W, AND SOMJEN GG. Current source density of sustained potential shifts associated with electrographic seizures and with spreading depression in rat hippocampus. *Brain Res* 570: 85–91, 1992.

YOUNG JN AND SOMJEN GG. Suppression of presynaptic calcium currents by hypoxia in hippocampal tissue slices. *Brain Res* 573: 70–76, 1992.

Downloaded from www.physiology.org/journal/jn by ${individualUser.givenNames} ${individualUser.surname} (129.034.020.019) on December 28, 2017.
Copyright © 2000 American Physiological Society. All rights reserved.